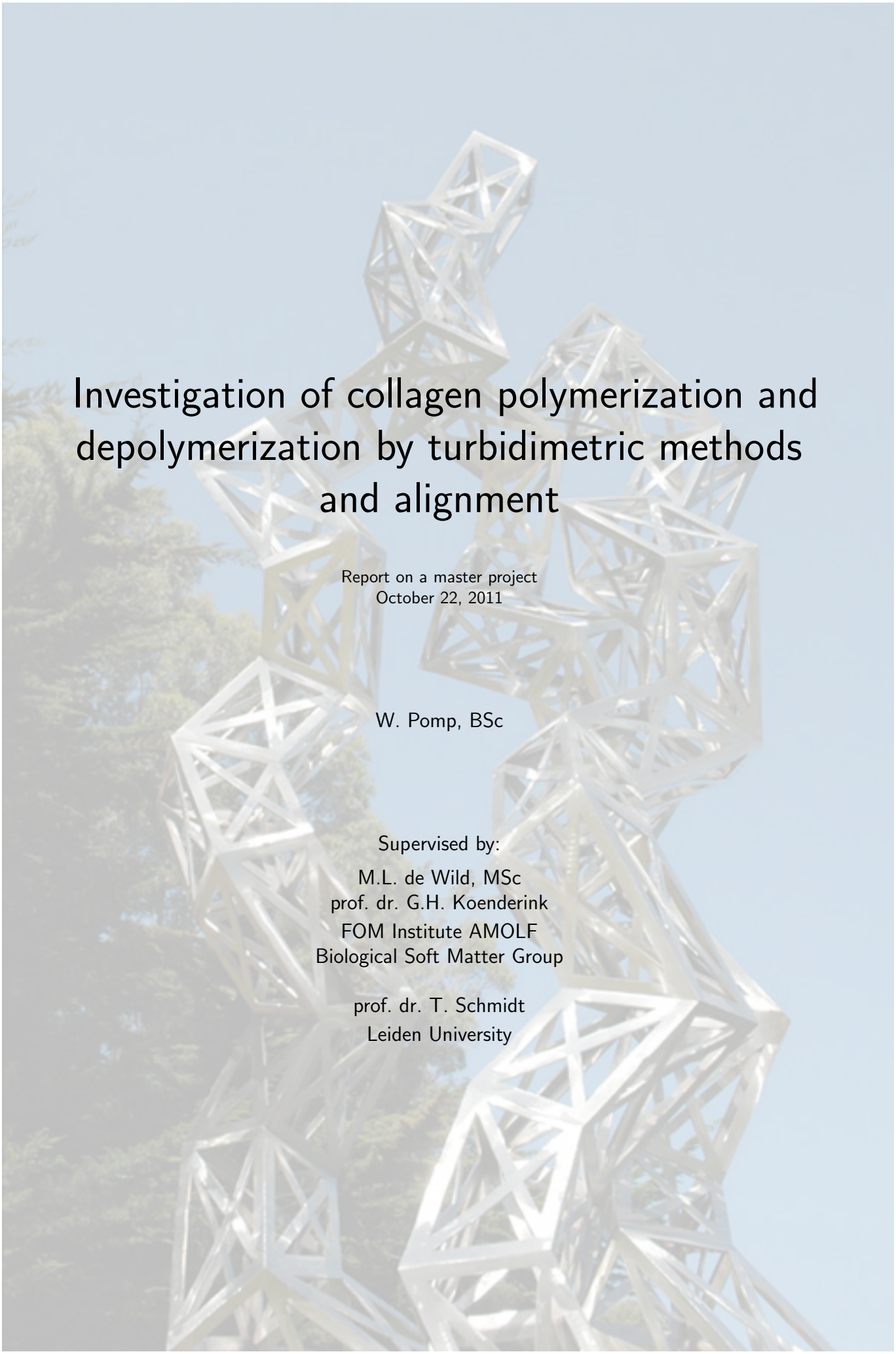

Investigation of collagen polymerization and depolymerization by turbidimetric methods and alignment

Report on a master project
October 22, 2011

W. Pomp, BSc

Supervised by:

M.L. de Wild, MSc
prof. dr. G.H. Koenderink
FOM Institute AMOLF
Biological Soft Matter Group

prof. dr. T. Schmidt
Leiden University

This report is written based on a five month internship at AMOLF for the master 'Research in Experimental Phyics' at Leiden University by Wim Pomp, BSc.
Email: wimpomp@gmail.com

Supervisors for this project were:

from AMOLF:
M.L. de Wild, MSc
prof. dr. G.H. Koenderink

from Leiden University:
prof. dr. T. Schmidt

Front cover image: Unraveling collagen, Julian Voss-Andreae

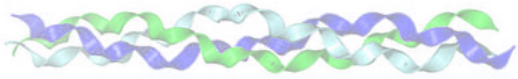

Abstract

The most abundant protein in the extracellular matrix is collagen. Upon heating to 37 °C, purified tropocollagen monomers in a neutralized solution spontaneously assemble into fibrils. This process is thought to be driven by an entropy gain of the water molecules. Measurements of the solution turbidity can reveal the kinetics of the assembly process since it reflects scattering by the fibers and depends on their number density and width. Prior turbidimetric experiments have shown that collagen polymerization proceeds via a nucleation-and-growth mechanism, whereby there is a lag phase in which the turbidity does not increase, followed by a sigmoidal increase of the turbidity due to fiber growth. Intriguingly, when the solution is cooled down to disassemble the fibers and then heated up again, there is no longer a lag phase. The goal of this master research project was to obtain better insight into the reversibility of collagen fibril formation when a fully formed network is brought to a lower temperature. To this end, two different experimental assays were developed. First, we attempted to align the collagen fibers during polymerization using a magnetic field or shear flow. The idea was that the degree of remnant collagen alignment after depolymerization and subsequent repolymerization might be a good reporter of the structures formed when the fibers are disassembled. Unfortunately, we were unable to obtain significant alignment of collagen based on collagens diamagnetism or even with embedded paramagnetic beads. Shear flow in a microfluidic channel also did not result in alignment, except for fibers on the surface. Therefore, this assay was abandoned. Instead, we used a second assay based on turbidimetry in a spectrophotometer with temperature control. These experiments showed that collagen polymerization showed a lag phase when the starter solution was a neutralized solution of tropocollagen, whereas polymerization of solutions obtained by cooling down an assembled network showed no lag phase. This suggests that nuclei capable of growing into fibers remain when the network is cooled down. The lower the final temperature, the lower the final turbidity of a collagen network after a temperature jump was, consistent with an association process that is at least partly reversible. However, we observed different depolymerization paths dependent on the rate of temperature decrease. This suggests nonequilibrium effects such as a changing shape of collagen fibrils upon depolymerization, a non-constant number of fibrils, and/or the spontaneous formation of crosslinks preventing full depolymerization.

Contents

1 Introduction

Many animals have a skeleton which provides structural integrity on a macroscopic scale. For solidity on cellular scales, animals have an extracellular matrix (ECM), which usually consists predominantly of collagens. Collagens form a large family, of which collagen types I, II, III, V and XI form fibrils. Of these, collagen I is the most abundant collagen.

It is known that purified collagen molecules in a solution of physiological pH and ionic strength self-assemble when the temperature is increased from 4 °C to body temperature [1]. This process can be (partly) reversed by decreasing the temperature again [2]. The polymerization process of collagen has been studied intensively since many years. However, there has been little research on the kinetics of the reverse process that occurs when a fully formed network is cooled down. It is known that there is a lag phase when a collagen is heated up to body temperature for the first time. During this lag phase, nuclei form which later grow into fibrils. However, it was shown that when a collagen network is depolymerized by cooling, there is no lag phase when the solution is reheated and the fibrils repolymerize. Apparently, fibril formation is not fully reversible.

The goal of this project was to study the temperature dependence of collagen polymerization and depolymerization to reveal mechanisms controlling the kinetics of these processes. Collagen networks were formed at different temperatures, and turbidimetry was used to measure the assembly rate and deduce the activation energy. Networks were then subjected to a quench to lower temperatures, and the turbidity was used as a measure of the degree of depolymerizaion. Moreover, we studied the dependence of collagen depolymerization on the rate at which the temperature was decreased. The nature of the fibrils that remain when a solution is cooled down is still unknown. To investigate whether the fibril network remains, we tried to develop an alignment assay which would allow us to measure remnant orientation after cooling/heating cycles, we tested three methods to align fibrils, involving either a magnetic field or a shear flow.

2 Turbimetric assays of collagen polymerisation and reversibility

2.1 Background

Tropocollagen molecules consist of three left-handed peptide strands twisted together in a right-handed coiled-coil helix with a length of about 300 nm and a diameter of 1.5 nm (see cartoon on the page header) [3]. Every third amino acid in a strand is glycine, the other two amino acids often are proline and hydroxyproline. When a solution of tropocollagen is neutralized and warmed up, the molecules spontaneously assemble into fibrils with a typical diameter of around 50 nm (figure 1). The packing arrangement of the molecules is highly periodic along the filament axis, with a precise quarter-stagger of neighboring molecules. These fibrils can associate laterally into fibers which in turn form a strong matrix in such places as bones, tendons and skin.

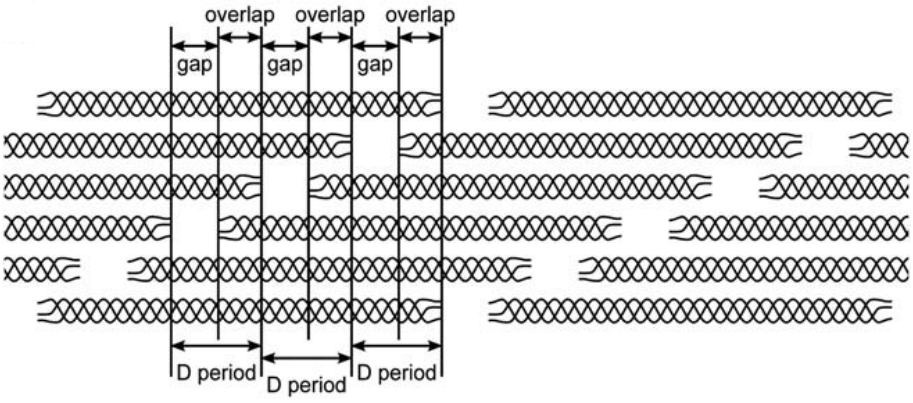

Figure 1: Axial packing arrangement of tropocollagen molecules in fibrils. The fibrils have a characteristic 67 nm D-period due to the precise quarter-staggered arrangement. Note that the drawing is not to scale since the molecules in reality have an aspect ratio of 200 [4].

2.1.1 Polymerization and depolymerization

X-ray diffraction experiments show a decrease in the lateral spacing between collagen molecules in fibrils as the temperature increases [5]. Collagen polymerization is thought to be driven by entropy [3, 5, 6]. A recent simulation study [4] shows that hydrophobic parts of collagen molecules restrict water molecules in their movements by not forming hydrogen bonds. The restriction in movements reduces the entropy of the system. Water molecules in a layer farther a way from the collagen experience less restriction. The entropy can be increased if collagen molecules move close to each other. This way the collagen molecules share layers of water, releasing some water in the bulk, and thus decreasing the entropy. Due to the distribution of hydrophobic and hydrophilic groups on the tropocollagen, the entropy is highest if the collagen molecules are displaced by about 67 nm to each other. In collagen fibrils this behavior leads to cross-sectional overlap and gap areas, shown in figure 1, the gap areas containing less collagen molecules than the overlap areas. In electron microscope images of negatively stained collagen fibrils such as the one shown in figure 2b this behavior is visible as darker and lighter regions.

Apart from entropy driven assembly, polar groups on protocollagen molecules also can have electrostatic interactions, other groups can form hydrogen bonds between protocollagen molecules. Since these bonds are non-covalent, collagen depolymerizes when the temperature is lowered [2]. If we assume that collagen polymerization is an equilibrium process then we can express the fraction of polymerized collagen at a given temperature T in terms of the change in Gibbs free energy, ΔG, in steady state:

$$p = \exp\left(\frac{\Delta G}{k_B T}\right) \tag{1}$$

Here k_B is the Boltzmann constant and $\Delta G = \Delta H - T\Delta S$, where ΔH and ΔS are the change in enthalpy and entropy, respectively. A larger change in the absolute magnitude of the Gibbs energy between depolymerized and polymerized states (which is negative for a spontaneous process), means that more collagen will assemble into fibrils. Given that the free energy is dominated by the change in entropy, increasing the temperature will lead to polymerization, while decreasing the temperature should lead to depolymerization.

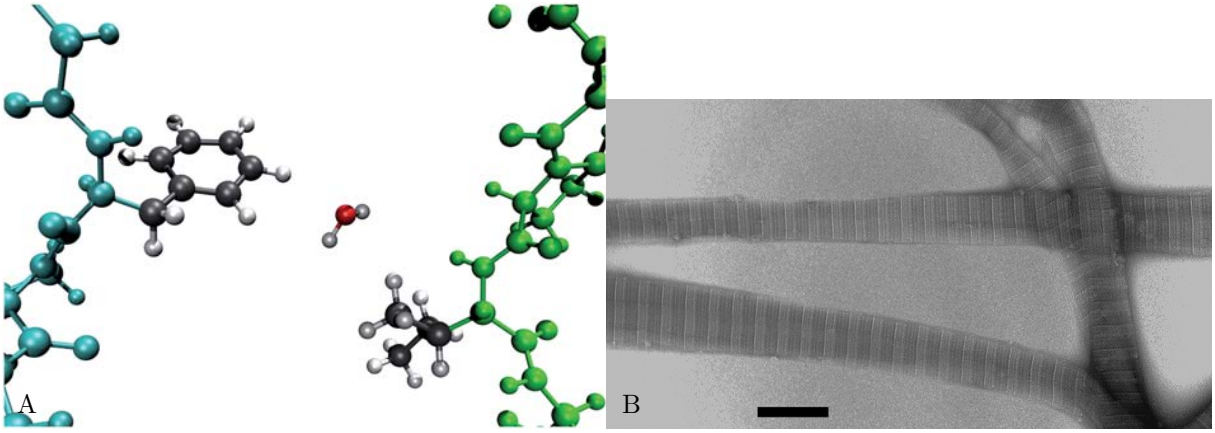

Figure 2: A. Two hydrophobic sidechains (black and white groups) on two collagen molecules (blue and green) share a water molecule (red oxygen atom and two white hydrogen atoms), decreasing the number of water molecules restricted in movements. [4]. **B.** Electron microscope image of collagen fibers formed from a solution of purified tropocollagen. The characteristic 67 nm D-banding is clearly visible as a zebra pattern on the negatively stained fibers. The scale bar is 200 nm. [7]

2.1.2 Turbidimetric experiments

Electron microscopy has been widely used in previous studies of collagen self-assembly. Turbidimetric assays offer an alternative way to probe the formation of collagen fibers, since the thick fibers scatter much more light than the small tropocollagen molecules. Since collagen fibrils are rod-like with a diameter smaller than the wavelength of visible light, we can use Rayleigh scattering theory to calculate the intensity of visible light scattered from a straight path through a collagen solution [8]. The amount of scattered light can be measured in a spectrophotometer from the amount of light transmitted through a cuvette filled with a collagen solution. The transmission is usually quantified by the logarithmic absorbance or extinction scale. The absorbance A is proportional to the concentration of collagen, provided that there is not multiple scattering [9]. The turbidity τ also depends on the path length, d, of the light through the sample [10]:

$$\tau = \frac{A}{d} \ln 10 = \frac{1}{d} \ln \left(\frac{I_0}{I} \right) \tag{2}$$

Here I_0 and I are the intensities of light, respectively before and after passing through the sample.

Turbidimetric experiments have shown the existence of a lag phase during collagen polymerization [1]. In fact there are theories describing the collagen polymerization process based on turbidimetric experiments [11]. Different parts of a turbidity curve of polymerizing collagen have been classified as lag, growth, or plateau phase [3, 12]. During the initial lag phase, there is no significant change in turbidity. The lag phase is followed by a growth phase in which the majority of the collagen is polymerized. Finally, there is the plateau, where nearly all of the collagen is polymerized, and the turbidity does not change anymore. The end of the lag phase and start of the growth phase are usually defined by drawing a tangent through the curve where the turbidity is half of the final, maximum turbidity [1]. Sometimes this is done with the time axis on a logarithmic scale, which is the procedure we adopt in this report. The end of the growth phase is defined in a similar way, as the time point at which the tangent intersects with a tangent to the plateau.

Depolymerization of collagen is much less well studied than polymerization. One study of Na [2] shows that collagen depolymerizes when the temperature is decreased, reaching a steady state with a temperature-dependent turbidity much lower than the original turbidity of the fibril networks. There is evidence that depolymerization is incomplete, possibly due to cross-links that form spontaneously during collagen polymerization. It has been shown that reduction of collagen with $NaBH_4$ can counteract cross-linking [2]. To investigate the reversibility of collagen polymerization we formed collagen networks at a fixed temperature of 37 °C and lowered the temperature. To study the dependence on the rate of cooling, we compared temperature jump experiments with slow cooling experiments at different rates.

2.2 Lag phase and growth kinetics

2.2.1 Lag phase

Earlier reports indicate the existence of a lag phase when collagen is polymerized for the first time by warming up a cold neutralized solution of purified tropocollagen [1]. This lag phase was shown to be absent during every subsequent polymerization following depolymerization. Turbidimetric experiments were done to confirm this behavior for a solution of pepsin-treated bovine dermal collagen. Figure 3a shows the time dependence of the turbidity of a solution of collagen at a concentration of 1 mg/ml during incubation for two hours at 37 °C. The curve shows the expected phases, with an initial lag time, followed by a rise of the turbidity and a plateau. However, we note that the turbidity is not constant in the plateau phase, but still increases slowly with time. To quantify the lag time we used a logarithmic fit (red line) to the data in the growth phase using the fitting equation $\tau = a - b\ln(t + c)$, τ and t being turbidity and time, and a, b and c are constants. The fit was performed for data points with turbidities $^1/_4$ and $^3/_4$ of the maximum turbidity (τ_{max}). The fitted line then was extrapolated down to the time axis to determine the delay between the start of the heating to 37 °C and the start of fiber growth. We have defined the period of this delay as the lag phase. Repeated measurements on 24 independently prepared collagen solutions gave lag times between 14 and 21 minutes, with an average of 17.7 ± 2.2 minutes.

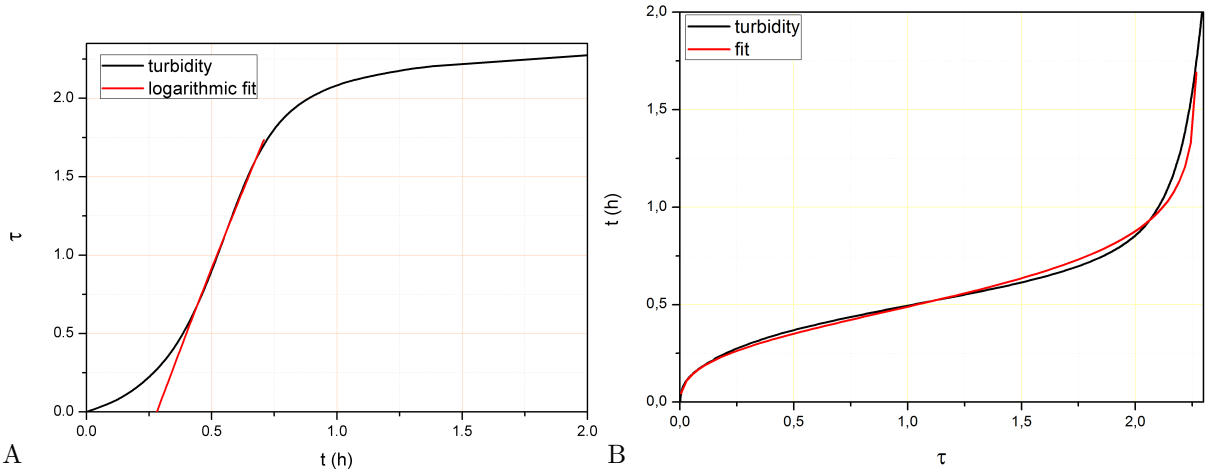

Figure 3: A. Turbidity of a polymerizing 1 mg/ml collagen solution at 37 °C (black line). The red line is a logarithmic function fitted between $^1/_4$ and $^3/_4$ of the maximum turbidity. Its intercept with the t-axis gives a lag time of 16.7 minutes. **B.** Time versus turbidity during the lag and growth phases in a 1 mg/ml solution polymerizing at 37 °C (black line). The data are fitted with equation 7 (red line).

Nucleation-and-growth model Wood & Keech [11] proposed a nucleation-and-growth model to describe the initial stages of collagen polymerization. During the lag phase collagen forms nuclei, which later grow in rod-shaped fibrils. It is assumed that after the lag phase, the shape and total number n_e of fibrils does not change significantly, and that the growth of these nuclei depends on their surface area $A \propto m^{2/3}$, and the concentration of tropocollagen c. So the increase in collagen mass m is given by:

$$\frac{dm}{dt} = k \cdot m^{2/3}(c - c_\infty) \tag{3}$$

Here c_∞ is the final collagen concentration. Defining the variables p and R:

$$p \equiv R^{1/3} \equiv \frac{c_0 - c}{c_0 - c_\infty} = n_e \cdot m \tag{4}$$

where c_0 is the initial collagen concentration, transforms equation 3 into:

$$\frac{dp}{dt} = k \cdot n_e^{1/3} \cdot (c_0 - c_\infty)^{2/3} \cdot p^{2/3} \cdot (1 - p) \tag{5}$$

upon integration Wood & Keech [11] arrive at the integral I which has a linear dependence on t:

$$I = \int \frac{dp}{p^{2/3}(1-p)} = \frac{1}{2}\ln\left(\frac{R^2 + R + 1}{(R-1)^2}\right) + \sqrt{3}\tan^{-1}\left(\frac{\sqrt{3}}{1 + 2R^{-1}}\right) = k \cdot n_e^{1/3} \cdot (c_0 - c_\infty)^{2/3} \cdot t \tag{6}$$

Here, k is the reaction rate constant, n_e is the number of collagen rods and c_0 and c_∞ are respectively the collagen monomer concentration before and after polymerization. Since there is a linear dependence of turbidity on collagen concentration: $p = \tau/\tau_{max}$. This equation accounts for the major features of the polymerization: lag and growth phases and a plateau. If this equation provides a full description of the process, then a plot of I versus t should give a straight line.

To fit equation 6 to our data we modify this equation with a parameter b to elevate the maximum turbidity to b^{-1}, and an offset t_0 to compensate for any delay between starting the measurements and heating the collagen solution. Furthermore, we define $A^{-1} \equiv k \cdot n_e^{1/3} \cdot (c_0 - c_\infty)^{2/3}$. So the equation fitted to our data, with A and t_0 as fit parameters and $b = \tau_{max}^{-1}$ is:

$$t = A\left(\frac{1}{2}\ln\left(\frac{(b\tau)^{2/3} + (b\tau)^{1/3} + 1}{((b\tau)^{1/3} - 1)^2}\right) + \sqrt{3}\tan^{-1}\left(\frac{\sqrt{3}}{1 + 2(b\tau)^{-1/3}}\right)\right) + t_0 \tag{7}$$

Figure 3b gives an example of such a fit for a turbidity curve measured during polymerization of a 1 mg/ml collagen solution at 37 °C; note that time is on the vertical axis and turbidity is on the horizontal axis. The resulting fit parameters are $A = 0.1967$ h $\pm 7.25175 \cdot 10^{-4}$ h, $b = 0.44$ and $t_0 = -0.0296$ h ± 0.00245 h; $\bar{R}^2 = 0.99469$, indicating that the equation describes the experimental data rather well. However, when the turbidity is nearing its maximum the model predicts a perfectly flat plateau, whereas in reality there is still a slow increase in the turbidity for a number of hours. In figure 4 turbidity curves measured at different polymerization temperatures between 28 and 37 °C are shown, plotted according to equation 6, with the time axis rescaled by lag time. During the lag and growth phases, portions of the graphs are approximately linear (see also the inset), especially at higher temperatures. However, after twice the lag time, which is when most of the polymerization is done, I is clearly not linear in time anymore. This indicates that the simple nucleation-and-growth model of Wood & Keech [11], which assumes that the fibril shape and number are constant, describes the lag and growth phases well, but fails at later times. Chapman [13] reported a maximum diameter for collagen fibrils, once this diameter is reached, growth only occurs at the ends of the fibrils. When this happens the nucleation-and-growth model does not hold since the shape of the fibril is not constant. Another possibility is that the packing density of the fibrils changes, changing the reaction rate by changing the interaction area, and possibly the turbidity by a changing refractive index of the fibrils.

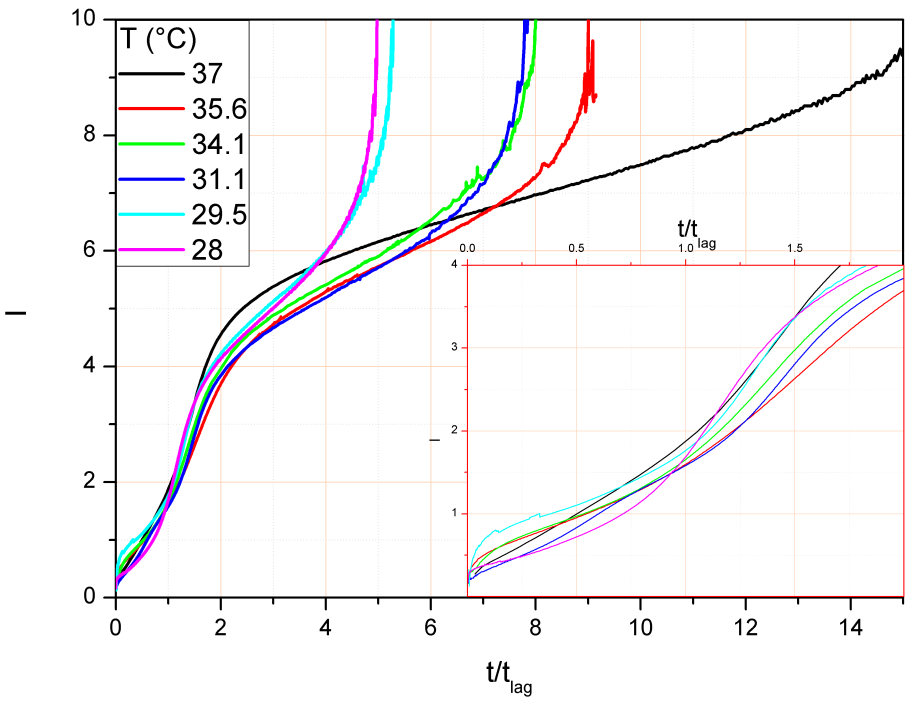

Figure 4: I versus time scaled to $t_{lag} = 1$, equation 6 suggests that this relation should be linear. The inset shows the first few hours. I has been calculated using data shown in figure 5a.

2.2.2 Dependence of polymerization kinetics on temperature

The rate of chemical reactions typically depends on temperature, and this dependence in general is described well by the Arrhenius equation:

$$k = A \exp\left(\frac{-E_a}{RT}\right) \tag{8}$$

relating the reaction rate k to the temperature T and the activation energy E_a. The activation energy is the energy barrier that the system needs to overcome [14]. A is a reaction specific constant and R is the gas constant. Collagen polymerization is not exactly a chemical reaction, but rather an entropy driven physical self-association [3]. Here we can still define an activation energy using equation 8 as:

$$E_a = -RT \ln {}^{k}/_{A} \tag{9}$$

We determined the activation energy for collagen assembly by measuring the polymerization rate of 1 mg/ml collagen at different temperatures between 28 and 37 °C from the time-dependence of the turbidity.

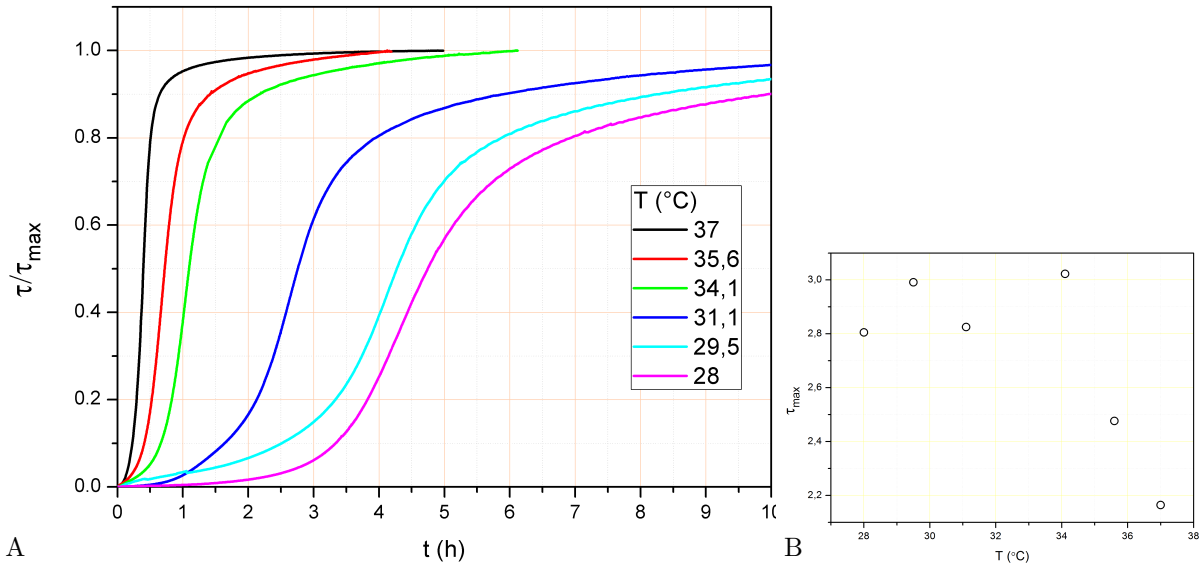

Figure 5: A. The rate of polymerization and the lag time for 1 mg/ml collagen solutions depend on temperature. The turbidities are normalized by the maximum turbidity which is measured as the turbidity some time after the plateau has been reached. **B.** Maximum turbidity as a function of temperature. Each measurement was performed once.

Figure 5a shows that the rate of collagen polymerization indeed increases with increasing temperature, whereas the lag time is strongly reduced. The turbidities are normalized by the maximum turbidities which where measured as the turbidity some time after the plateau has been reached. As shown in figure 5b the maximum turbidity decreases somewhat with increasing temperature. Since the polymerization at lower temperatures takes much longer, it could be that during that time another process going on, resulting in a higher turbidity.

As shown in figure 6a, the polymerization rate follows the expected Arrhenius dependence on temperature, with a linear dependence of $\ln k$ on ${}^{1}/_{T}$. The slope gives an activation energy of 43 kcal/mole, which is comparable to values reported in earlier reports. Bensusan & Hoyt [15] report activation energies between 23 and 51 kcal/mole for bovine dermal collagen solutions with different added ions, whereas Wood & Keech [11] report an activation energy of 40 kcal/mole for a 1 mg/ml bovine dermal collagen solution in a 0.5 mg/ml sodium acetate buffer. However both Bensusan & Hoyt [15] and Wood & Keech [11] use collagen which is not pepsin-treated.

If the polymerization process during lag and growth phases is the same, then the activation energy during growth and lag phases is the same. And since in an activation energy calculation any constants preceding $k(T)$ drop out, $k_{growth}(T)$ should be proportional to $k_{lag}(T)$. According to figure 6b the lag time seems to scale well with the growth time or ${}^{1}/_{k} \propto t_{lag}$. As expected, the inverse rate scales linearly with lag time (figure 6b).

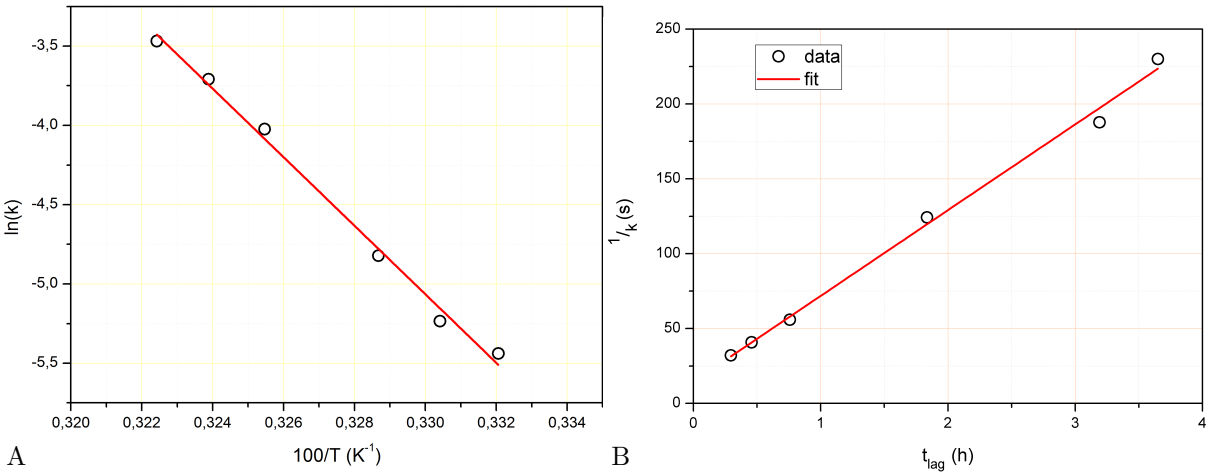

Figure 6: A. Van 't Hoff plot of collagen polymerization, the activation energy calculated from the slope of the fit is 43 kcal/mole. **B.** Polymerization rates determined from the turbidity data shown in figure 5a, k was measured when $\tau = {}^1/_2\tau_{max}$. Lag times are determined according to the earlier described method of extrapolating the growth phase down to zero turbidity.

2.3 Reversibility of collagen polymerization

2.3.1 Turbidity response to temperature jumps

Since collagen molecules interact by non-covalent interactions, collagen polymerization is expected to be a reversible process, which is temperature dependent. Collagen is expected to polymerize upon heating, and to depolymerize upon cooling. However, there is evidence from turbidimetric measurements that polymerization is not entirely reversible. The main evidence is the absence of a lag phase when collagen is repolymerized by reheating [1]. Apparently, some collagen remains in oligomer or fibril form, possibly due to the presence of spontaneously formed crosslinks. To probe the temperature dependence of collagen depolymerization, we measured the response of the turbidity of a 1 mg/ml collagen fibril network formed at 37 °C to a fast temperature jump from 37 to 12 °C.

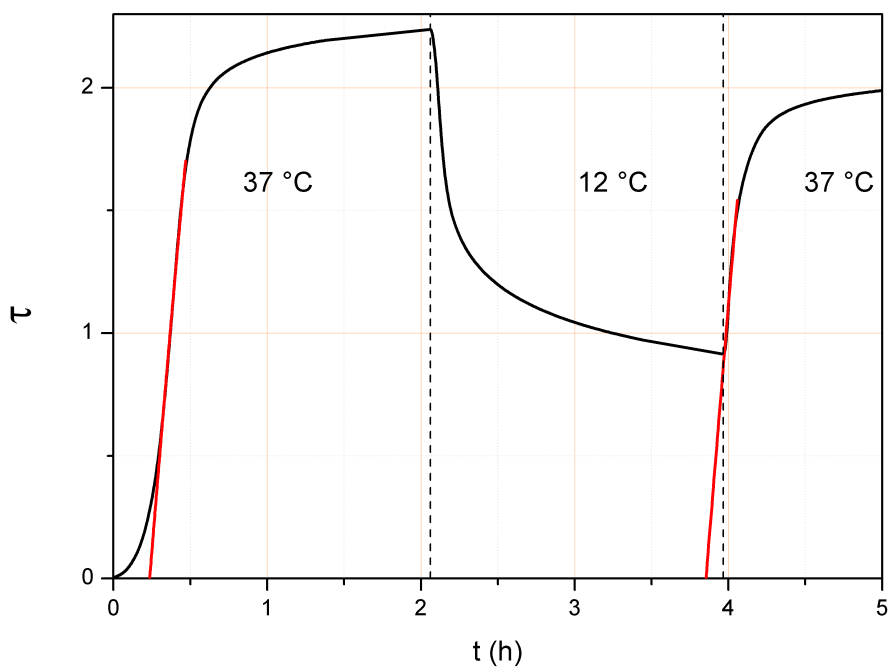

Figure 7: Turbidity of a 1 mg/ml collagen sample during cycles of heating for 2 hours to 37 °C and cooling for 2 hours at 12 °C (black line). The temperature is rapidly switched as indicated by the dashed lines (the switch takes about 2 minutes). Red lines are logarithmic functions fitted between ${}^1/_4$ and ${}^3/_4$ of the maximum turbidity. Their intercepts with the t-axis give lag times. On the heating step at $t = 0$ there is a lag phase of about 15 minutes, whereas on the second heating step at $t = 4$ hours the turbidity starts to rise immediately.

As shown in figure 7, the turbidity of a 1 mg/ml collagen solution increases after a lag phase, when the sample is heated to 37 °C. It decreases again when the temperature is lowered (which takes approximately

two minutes) to 12 °C. The turbidity drop appears to be biphasic, with an initial fast decrease followed by a slower decrease. When the collagen is again heated to 37 °C, after an incubation of 2 hours at 12 °C, the turbidity rises immediately without a lag. This suggests that after depolymerization, nuclei remain in solution. These nuclei may be oligomers or even fibrils. Note that the turbidity reached in the second polymerization step at 37 °C is lower than the turbidity reached in the first step.

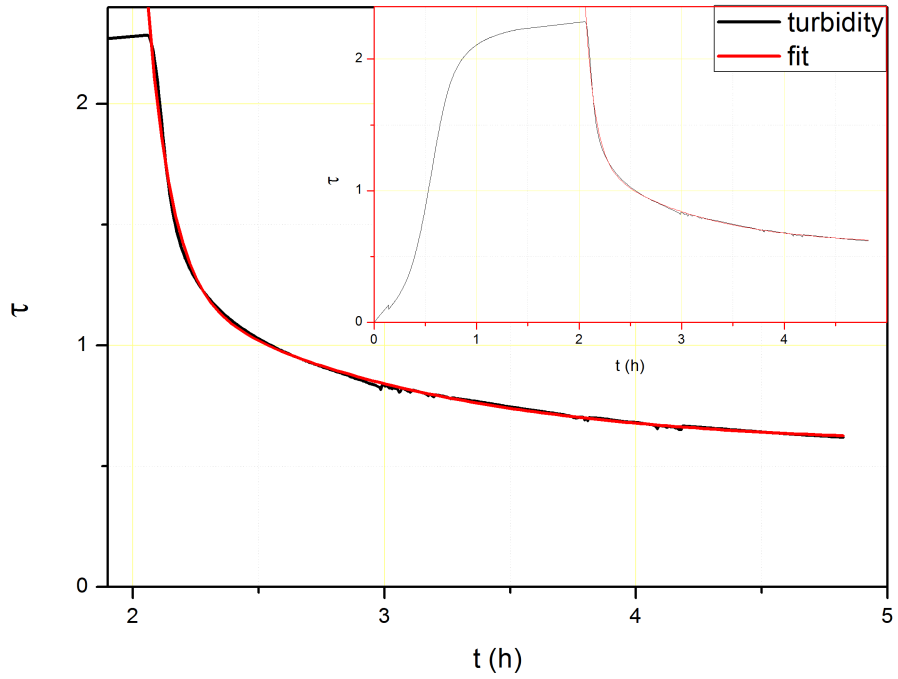

Figure 8: Turbidity of a 1 mg/ml collagen solution during depolymerization (black line). The temperature is lowered from 37 to 12 °C at $t = 2$ hours. The red line is a double-exponential decay fitting function. The asymptote of this function is taken to be the turbidity at infinity. The inset shows the same data, but also includes the rise in turbidity during polymerization at 37 °C between $t = 0$ and 2 hours.

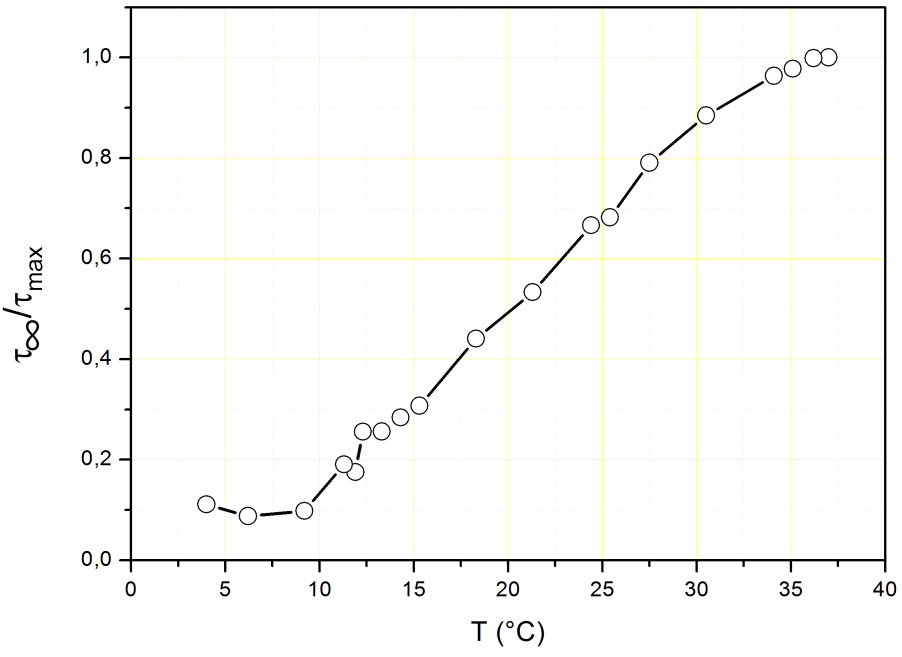

Figure 9: Fraction of remaining turbidity after once polymerized collagen has been depolymerized for 2 hours at a given temperature. Each point represents one experiment.

Temperature dependence of reversibility For an equilibrium assembly process, the amount of fibrils in equilibrium with monomers should decrease with decreasing temperature. To test this prediction, we polymerized 1 mg/ml solutions at 37 °C for two hours, which is sufficient to reach nearly complete polymerization. In the literature, it is generally claimed or assumed that the turbidity is constant after two hours [1], though we still observe a slow increase of turbidity over time (figure 8). After network formation, the temperature was lowered to a temperature between 37 and 4 °C within approximately two minutes. An example of such an experiment is shown in figure 8. The resulting turbidity response

was then fitted to a double-exponential decay with two time constants (red line in figure 8:

$$\tau = A_1 e^{t/t_1} + A_2 e^{t/t_2} + \tau_\infty \tag{10}$$

Here, τ_∞ is the minimum turbidity to which the turbidity is decreasing. One long experiment which ran for another 20 hours after the usual 3 hours after the temperature drop, showed that the turbidity actually decreases below t_∞ another 2.3%. However, since this difference is small and since longer experiments are impractical, we used the value of τ_∞ as the steady-state value. As shown in figure 9, the steady state value of the turbidity relative to the maximum turbidity of the gel at 37 °C decreases steadily with decreasing temperature. This dependence is consistent with an entropy-dominated assembly process.

Activation energy for depolymerization As explained in section 2.2.2, the rate of polymerization of collagen as a function of temperature reveals the activation energy for assembly. For reversible chemical reactions there usually also is an activation energy E_b for the reverse reaction. A diagram of this is displayed in figure 10. On the path from monomer to polymer or vice versa, the reaction has to overcome an energy barrier. The size of this barrier is E_a upon polymerization, and E_b upon depolymerization. The difference between E_b and E_a is the standard enthalpy of formation: $\Delta G^\circ = E_a - E_b$. The Gibbs free energy is related to this as follows: $\Delta G = \Delta H - T\Delta S = \Delta G^\circ + k_B T \ln p$. Given that ΔG° is constant this yields:

$$p = \frac{k_a}{k_b} = A \cdot e^{\frac{\Delta G}{k_B T}} \tag{11}$$

where p is the fraction of collagen in polymer form, and $A = \exp\left(-\Delta G^\circ / k_B T\right)$. Therefore, the slope of a graph where $\ln p$ versus $1/T$ is plotted, should yield the Gibbs free energy. We do not know the fraction of collagen in polymer form, since the turbidity is only an indirect measure. The turbidity depends on the concentration of fibers, as well as on their diameter and mass-length ratio. As shown in figure 11, the natural logarithm of the ratio between τ_∞ and τ_{max} does not depend linearly on $1/t$, but rather scales as $\ln p \propto -1/T^2$. If the turbidity ratio does represent the fraction of polymeric collagen, then this result suggests a Gibbs free energy which is dependent on $\exp 1/T^\beta$ with $\beta > 1$. This would imply, given that entropy dominates, that the change in entropy upon depolymerization itself is dependent on temperature. However, other experiments probing the fraction of collagen in polymeric form more directly (for instance by sedimentation assays) will be needed to clarify this issue.

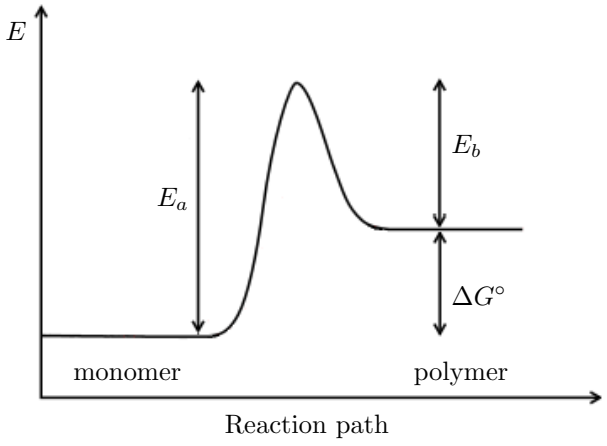

Figure 10: Diagram of the energy along the reaction path. On the reaction from monomer to polymer or back, an energy barrier must be overcome. The size of this barrier is E_a upon polymerization, and E_b upon depolymerization. The difference is the standard enthalpy of formation: $\Delta G^\circ = E_a - E_b$.

2.3.2 Dependence of collagen depolymerization on cooling rate

For depolymerization to reach an equilibrium, sufficient time is needed, as shown by our data in section 2.3.1. To test how depolymerization is affected by cooling rate, we again polymerized collagen at a concentration of 1 mg/ml and temperature of 37 °C for two hours. However, now the temperature was decreased to 4 °C in periods varying from 15 minutes to 96 hours. An infinitely slow cooling rate should allow the system to approach equilibrium adiabatically. As shown in figure 12, the rate of cooling affects the final turbidity reached by collagen samples cooled down to 4 °C. Turbidity curves obtained for slow cooling over periods of 24 or 96 hours overlap, showing a gradual decrease with decreasing temperature, suggesting that collagen depolymerization is very near to an equilibrium at all temperatures. Samples cooled down more quickly, over periods of 8 or 16 hours, have turbidity curves that are somewhat lower.

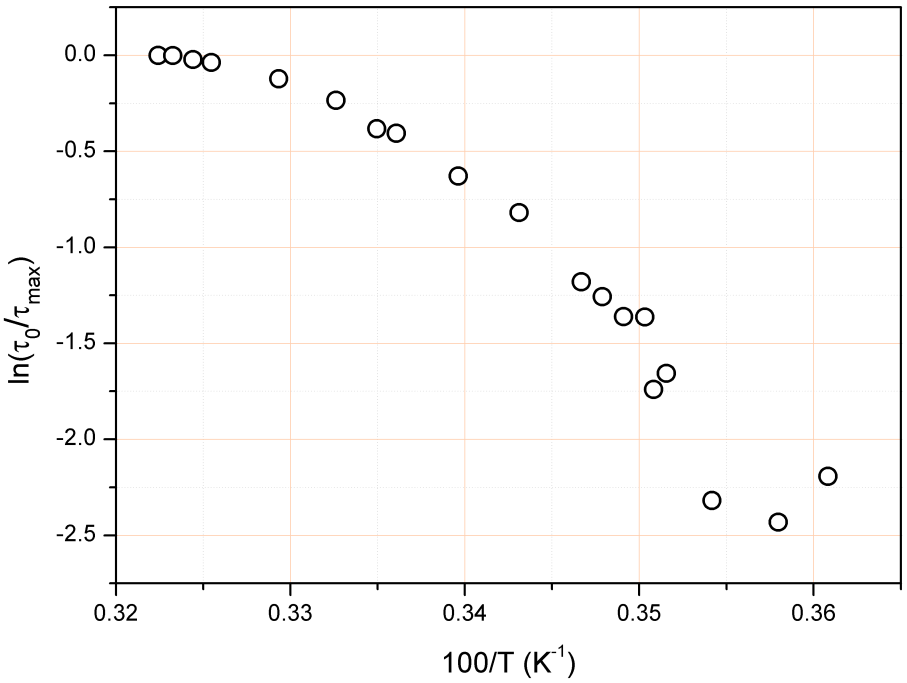

Figure 11: Van 't Hoff plot of the temperature-dependent turbidity of collagen samples after depolymerization, relative to the initial turbidity of the network at 37 °C (data from figure 7). This plot is expected to be linear if the turbidity ratio is proportional to the amount of polymeric collagen and if the Gibbs free energy is not temperature dependent.

But still show a gradual decline with decreasing temperature. In contrast, samples cooled down rapidly in 30 or 15 minutes, show a precipitous drop of the turbidity when the temperature falls below 37 °C.

Let us assume that for every temperature there is a fixed equilibrium in collagen polymerization. Then this equilibrium would not depend on how fast the temperature decreases, and the curves in figure 12 would all be similar. When a certain temperature is reached it takes some time, depending on the cooling rate, before the corresponding equilibrium is reached. Therefore, the only difference between these curves would be that curves corresponding to a faster cooling would be shifted to the left relative to the curves with a slower cooling. However, the curves in figure 12 corresponding to cooling from 37 to 4 °C in 15 and 30 minutes have a different shape from, and are below the curves corresponding to a slower cooling. So the collagen depolymerization is temperature path dependent. A possible explanation is that there is more than one mechanism involved in depolymerization of collagen.

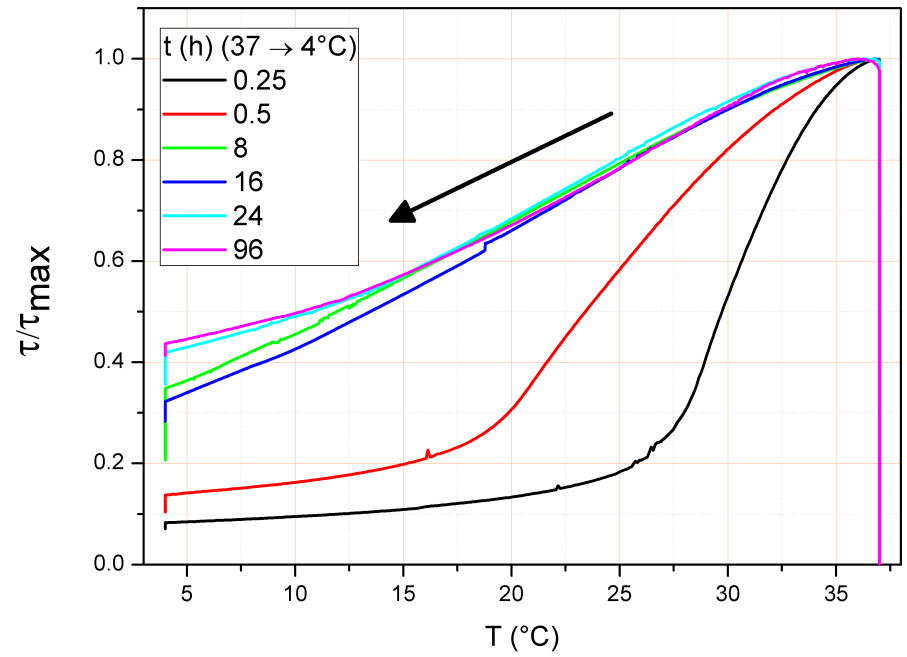

Figure 12: Turbidity versus temperature for 1 mg/ml collagen samples. The collagen has polymerized for 2 hours at 37 °C, after that, the temperature was slowly decreased to 4 °C in different amounts of time (indicated in the legend).

Mechanisms In section 2.3.2 we suggested that is more than one mechanism involved in collagen depolymerization. Which different mechanisms these are is not clear from this experiment. A hypothesis is that detachment from a collagen fibril has different rates for molecules on the sides or on the ends of the polymer, depending on temperature. This would yield different paths of depolymerization, like in figure 12. However, all these paths would give the same amount of polymerized collagen if the collagen is incubated for a long time at 4 °C after the temperature decrease is stopped.

Already in section 2.3.1 we saw that there are multiple processes going on during polymerization. After the majority of collagen is polymerized, the turbidity is still increasing (figure 8). In our experiments in section 2.3.1, collagen did not depolymerize to the same level as before polymerization. Na [16] suggested that covalent cross-linking in fibrils probably is the cause of this. If this process also occurs during depolymerization, then it makes a difference how fast collagen depolymerization happens. This process would not play a major role in short depolymerization experiments, for example the ones in which the temperature is decreased from 37 to 4 °in less than 30 minutes in figure 12. It would however, occur in longer lasted experiments, in which it increases the turbidity over time. If this hypothesis is to explain figure 12 then the turbidities of the different curves in figure 12 should not reach the same turbidity when the collagen is incubated a long time after the temperature decrease has been stopped.

2.3.3 Repolymerization from depolymerized collagen

In figure 7 it is visible that the turbidity does not return to its former maximum after the collagen has been depolymerized and repolymerized. To investigate the dependence of reversibility on the number of depolymerization cycles, we did an experiment in which we subsequently polymerize and depolymerize collagen for two hours at 37 and 4 °C respectively. As can be seen in figure 13a, and figure 13b, where the peaks from figure 13a have been plotted, on every subsequent polymerization the maximum turbidity gets lower. Between the first two peaks there is large drop in turbidity, on every subsequent step the turbidity gets lower. This could be due to collagen becoming unable to polymerize again, for example by forming oligomers. The molecules in these oligomers do not cooperate in the process of repolymerizing fibrils again, but are too small to have any major effect on the turbidity. This hypothesis has not been tested yet. An alternative explanation is that the shape and packing density of collagen fibrils is different every time the collagen is repolymerized.

Since collagen polymerization and depolymerization are equilibrium processes, molecules are added to and removed from the fibrils all the time. What our results suggest is that while in equilibrium the total amounts of molecules added and removed from the fibrils may be equal, the amounts added to, and removed from the sides versus the ends may not be equal. This way collagen molecules are transfered from the ends of a fibrils to the sides or vice versa, setting a new equilibrium. Earlier reports indicate that a collagen fibril has a maximum diameter [3, 13]. When most of the growth stops when that diameter is reached, the fibers can get shorter or longer on every subsequent depolymerization and repolymerization, depending on the ratio of growth rates for polymerization on the sides or ends of fibrils.

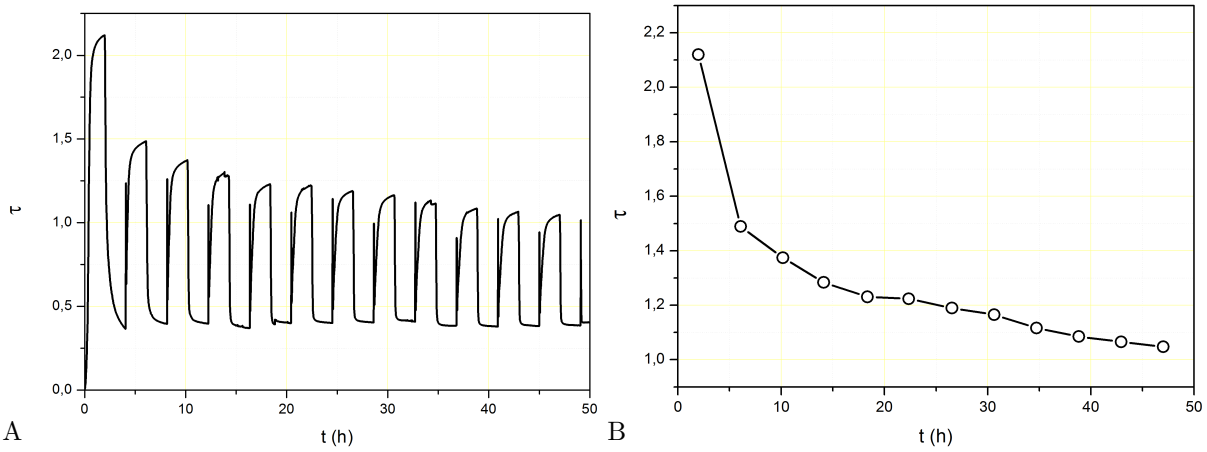

Figure 13: A. Turbidity does not get back to the same level upon subsequent polymerization and depolymerization for two hours each at 37 °C and 4 °C respectively. **B**. Peaks from figure 13a plotted. There is a large drop in turbidity between the first and second peak, after that each peak is a little lower.

2.4 Conclusion

2.4.1 Kinetics

Collagen polymerization shows a lag phase when collagen is polymerized for the first time. Furthermore, the length of this lag phase depends on the temperature at which polymerization occurs. Wood & Keech [11] proposed a nucleation-and-growth model to describe both the lag and growth phases. Our turbidity curves measured over a range of different temperatures can be rescaled on top of each other in the lag phase and most of the growth phase in accordance with the model (figure 4). However, the data deviate from the model predictions at later times. This indicates a violation of at least one of the assumptions made in the modeling, for instance the assumption that the number of fibrils, length to thickness ratio or density of molecules in a fiber are constant.

2.4.2 Reversibility

The degree of depolymerization also depends on temperature: assuming that the turbidity is representative of the amount of polymeric collagen, then the polymerized collagen is reversible to about 10 to 15% of the amount polymerized at 37 °C when the temperature is reduced to 4°C. The remaining fibrils may be irreversible due to crosslinking. The reversibility strongly depends on the rate at which the temperature change occurs. We have shown that when decreasing the temperature slowly, the depolymerization takes another path. The absence of a fixed equilibrium in collagen polymerization for a certain temperature suggests that there is more than one mechanism involved in collagen depolymerization. We do not know which mechanisms are involved, but our hypothetical mechanisms involve a variable shape of collagen fibrils.

2.4.3 Outlook

The conclusions above call for a method to measure other variables besides the fraction of polymerized collagen. Turbidity measurements may be carried out at different wavelengths to determine mass per length and radius, and thus indirectly, density of the collagen fibrils [10, 17]. Other possible methods to measure the radius and morphology of the collagen fibrils include AFM and electron microscopy.

3 Development of a new assay of collagen reversibility by alignment

3.1 Background

Often the fibers in extracellular matrices are aligned with each other, such as in the cornea. Many researchers have tried to artificially align collagen fibers, with varying success. Different methods have been applied including flow alignment [18–22], an electrochemical method [23], alignment by electro spinning [24–26] and strain induced alignment methods, either on a macroscopic scale [27], or on a microscopic scale by AFM [28]. Furthermore, alignment was previously induced by means of magnetic fields, either directly by very strong magnetic fields [29], and even by relatively weak magnetic fields [30], or indirectly by inducing flow by pulling magnetic beads through a collagen solution [31].

Usually, the goal of collagen fibril alignment has been to design methods to replicate tissues. In contrast, our goal is to use collagen alignment as an assay for the behavior of collagen when polymerizing. Turbidimetric experiments prove that when polymerizing fresh collagen there is a lag phase which is absent on every subsequent polymerization [2]. During this lag phase the turbidity does not notably change [12], but there are still processes going on that contribute to polymerization. When collagen is depolymerized these processes are not reversed. When collagen is polymerized, it could be that it returns to a state in which only small nuclei are left [11], or to a state in which there are only very thin fibers left. These nuclei or this network is then preserved during successive depolymerization and polymerization steps. Because nuclei randomly reorient every time by Brownian motion, and fibers in a matrix do not, we can establish which of these hypotheses is correct by aligning collagen before its first polymerization, and determining the direction of orientation and degree of anisotropy after each time the collagen is polymerized. The orientation and anisotropy can be calculated by analyzing microscope images [30].

We first attempted to align collagen fibrils in a magnetic field. Paramagnetic materials become magnetic in the presence of a magnetic field and will be attracted by a magnet held close to it. Diamagnetic materials also become magnetized, but produce a field opposite to the externally applied field and are repelled by magnets. Among the common weakly diamagnetic materials are water, copper and carbon. Collagen also is weakly diamagnetic [29, 32]. Also, there is an anisotropy in the magnetic susceptibility of collagen so that the field strength of the field produced depends on the orientation of the collagen in the applied field. Collagen is most susceptible to magnetic fields along its axis [29,32]. This makes that collagen fibrils tend to align perpendicular to strong magnetic fields [32]. We tried to align collagen by magnetic fields generated by permanent magnets, in a field of about 1 T.

Other magnetic experiments were based on superparamagnetic beads, which are attracted by a magnet. The force on a magnetic bead depends on its magnetization, and the gradient in the magnetic field of the magnet [33]. By putting these beads in polymerizing collagen samples, we tried to align the collagen fibrils during their formation. As an alternative method we also used a lamellar flow to align collagen in a microfluidic channel.

3.2 Magnetic alignment based on collagen diamagnetic properties

Several attempts were made to align collagen in a simple way using magnetic fields. Since collagen is a weakly diamagnetic material, it tends to align orthogonally to a magnetic field [32], the energy cost to be unaligned being $^1/_2 \cdot N\chi B^2$. Here, B is the magnetic field, N is the number of collagen molecules in a fibril and $\chi \approx -10^{-25}$ JT^{-2} is the magnetic susceptibility per collagen molecule.

The number of fibrils with a given orientation is given by a Boltzmann distribution, for he fraction of collagen fibrils aligned orthogonal to the magnetic field this yields [32]:

$$1 - \exp\left(\frac{-NB^2\chi}{2k_BT}\right) \tag{12}$$

Here N is the number of collagen molecules in a fibril. If this number is as low as 1000 in a 1 T field this yields an anisotropy of only 1.2% more fibrils orientated perpendicularly than parallel to the magnetic field. However, when N is larger, the number of aligned fibrils should grow rapidly, being 70% for fibrils about 25 µm long and 50 nm in diameter, such as in figure 14. However, fibrils only orient if they are not restricted in their motion. Most of the collagen fibrils in our dense solutions (1 mg/ml), however, form networks, and probably are attached to other fibrils before having grown large enough to have a significant preference in orientation.

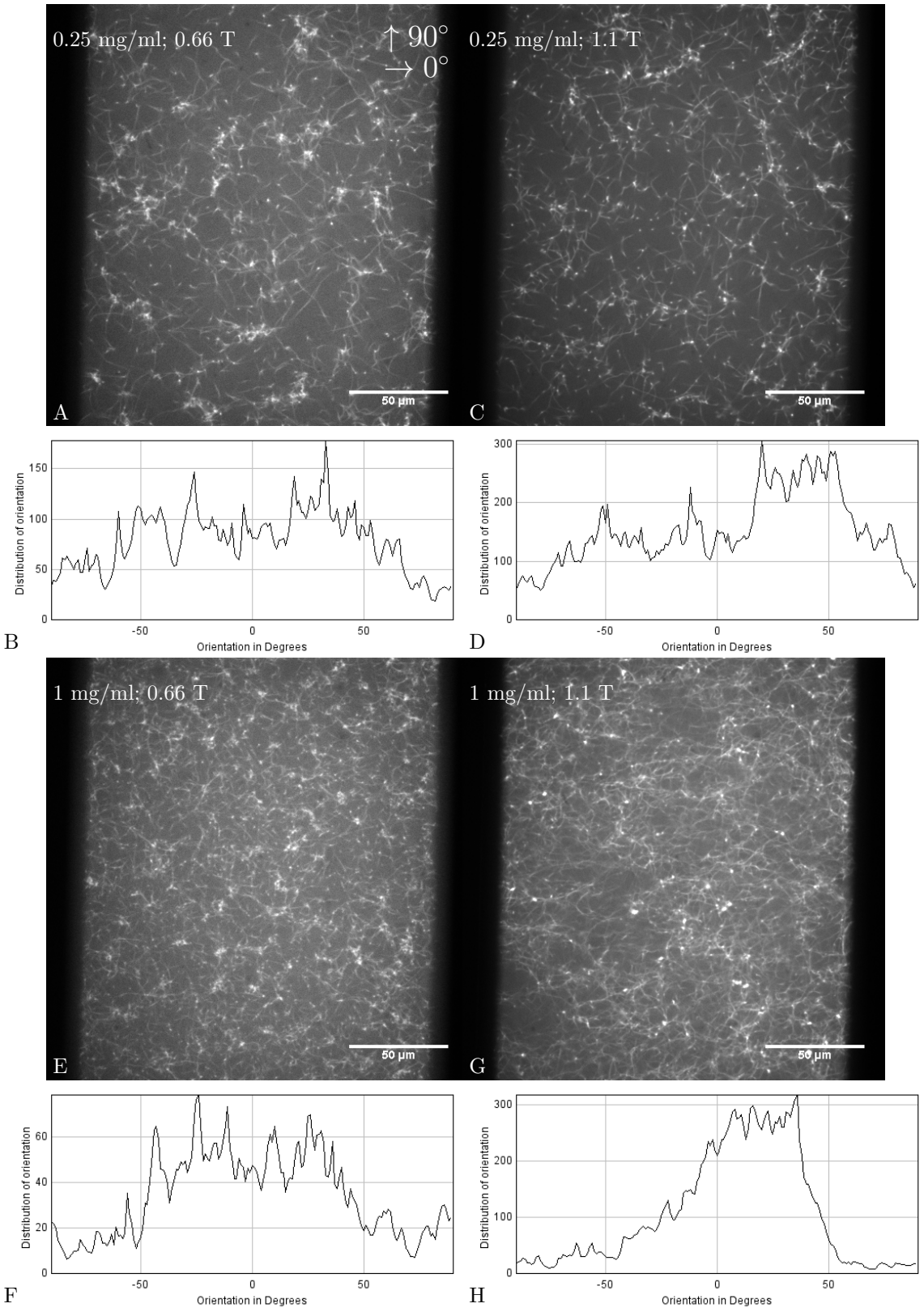

Figure 14: Collagen at concentrations of 0.25 mg/ml and 1 mg/ml polymerized in magnetic fields of 0.66 T and 1.1 T. **B**, **D**, **F** & **H** are histograms of the pixel orientations in panels **A**, **C**, **E** & **G**, obtained using the plugin OrientationJ in ImageJ. In all pictures the magnetic field is horizontal (0°) and the collagen fibrils should be aligned vertically (90°).

Alignment of collagen has been reported in strong magnetic fields of 7 T [29] and even in a comparatively weak field of 0.7 T [30]. We used fields up to 1.1 T and solutions of 1 mg/ml collagen. However, since fibrils in samples with high concentrations can be prohibited from orienting in the magnetic field by binding with other fibrils, concentrations as low as 0.1 mg/ml and as high as 5 mg/ml were also tested. Fibrils in low concentrations touch less other fibrils. We reasoned that at high concentrations fibril alignment might be promoted because parallel alignment is the most volume-efficient way of packing fibrils. In a few experiments the collagen was in a 10 μm thick chamber, where confinement effects might promote collagen fibril alignment by the magnetic field. The magnetic field was always in the plane of the glass (xy-plane), so that alignment would also occur in the xy-plane, but perpendicular to the magnetic field. The images taken by confocal microscopy were then analyzed using the OrientationJ plug-in for ImageJ, which calculates the orientation of every pixel in an image by comparing its brightness to that of its neighbors.

Although some anisotropy is visible in most images from collagen polymerized in a magnetic field, like in the examples in figure 14, the direction of alignment is in the direction of the magnetic field, contrary to our expectations. Furthermore, images of control samples polymerized in the absence of a magnetic field (other than the Earth magnetic field), do not show significantly different anisotropies. However, on average the samples showed some anisotropy in the unexpected direction along the magnetic field lines. This possibly stems from the fact that while the top and bottom of the sample were sealed with parafilm, the sides were sealed with the less rigid silicon grease. Upon heating, the sample then may expand mainly towards the sides, stretching the network, and thus causing apparent slight anisotropy.

3.3 Magnetic alignment using paramagnetic beads

Another method relying on magnetic beads was also tried, inspired by recent papers where beads were shown to move in the direction of the highest magnetic field density, thereby inducing a flow and pulling on the collagen [31, 33]. Again, experiments were done using collagen concentrations between 0.1 and 5 mg/ml. Different magnets pulling the beads with different forces were used. A small magnetic stir bar producing about 0.1 T at its poles was placed on top of a pile of samples as drawn in figure 15a. In other experiments, cylindrical magnets 10 mm in diameter were placed on top of the pile of samples or next to it, the farthest sample being about 10 cm apart from the magnet. This experiment was also repeated using a bar magnet producing a stronger magnetic field of about 0.4 T at its poles. Also in some of these experiments the magnet was positioned near the sample only after the lag time, to prevent the magnetic beads from arriving at the magnetic poles before the collagen was polymerized.

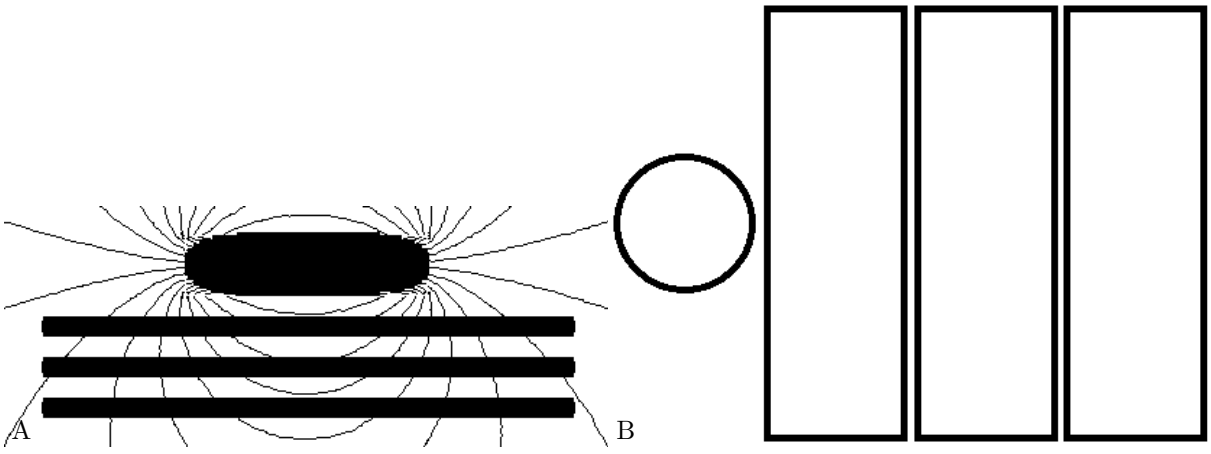

Figure 15: A. Magnetic stir bar lying on top of a pile of samples so that the force on the magnetic beads in the samples becomes smaller the lower the sample is in the pile. There was about 3 mm between the samples. **B.** The same idea as in the left picture, but now using a bigger magnet, the 26 mm wide slides are next to each other this time.

Adding superparamagnetic beads to the collagen solution and pulling them with various magnets while the collagen polymerizes yields approximately the same results as the diamagnetic method does. There is sometimes some fibril alignment, but as before, their number is insignificant and/or in the wrong direction. Figure 16 shows three images from samples of which the first one was next to a 10 mm diameter magnet, generating about 0.5 T at its surface. The second and third are from samples next to that, according to

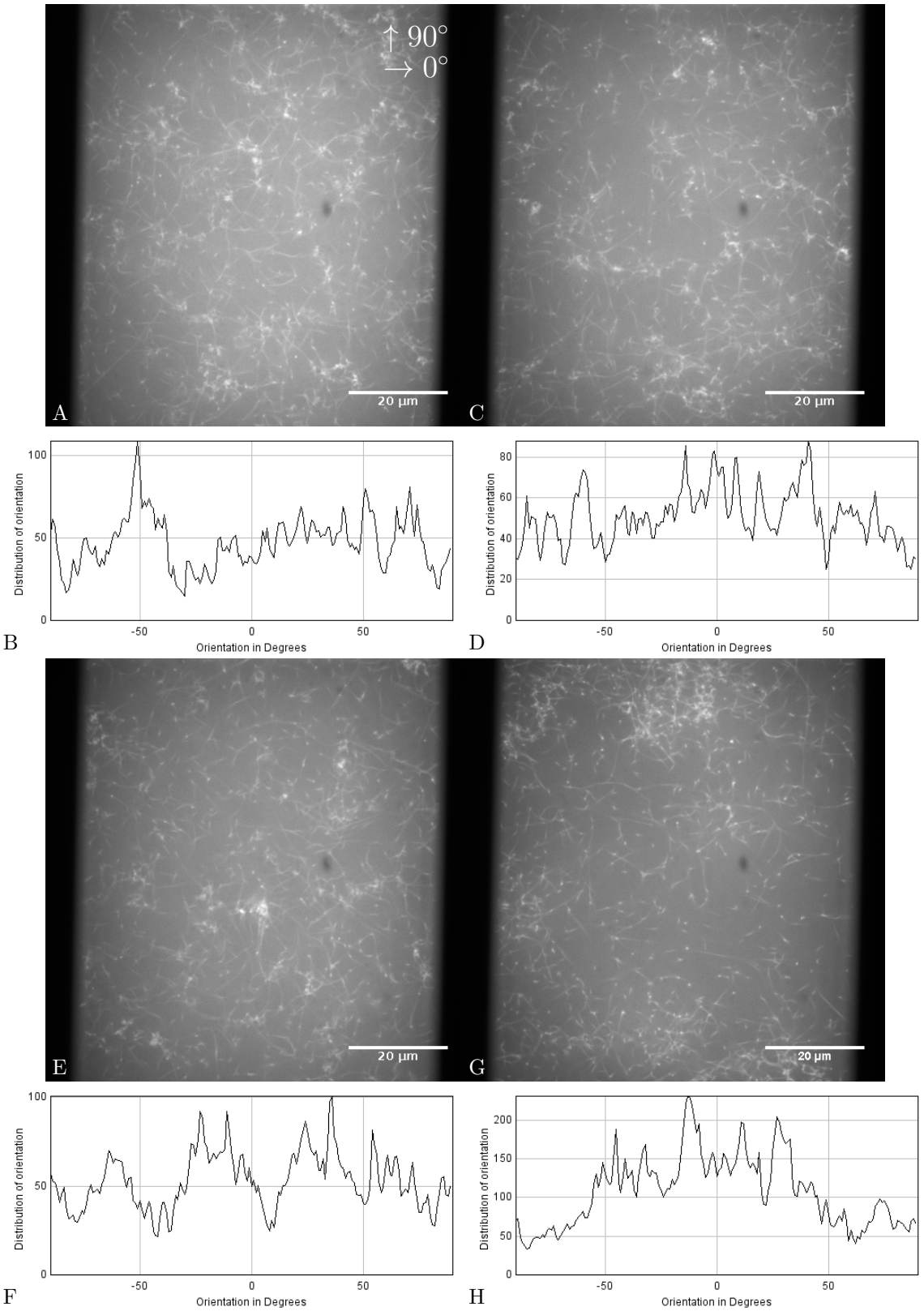

Figure 16: Collagen polymerized at a 1 mg/ml concentration in the presence of $5 \cdot 10^4$ ml^{-1} magnetic beads. **A** is next to the magnet, **C** is next to that and **E** is farthest away (about 6 cm). In **G** there were no magnetic fields present. **B**, **D**, **F** & **H** are histograms of the pixel orientations in **A**, **C**, **E** & **G**, obtained using OrientationJ. In all pictures the magnetic field is horizontal (0°) and the collagen should be aligned vertically (90°).

the arrangement as in figure 15b. In these images no alignment is seen at any distance from the magnet. The fourth image, which is from another set of experiments, was far away from any magnet and serves as a control. In this control there are also slightly more fibrils aligned horizontally than vertically. It is obvious from this control that the apparent alignment does arise also without any magnetic fields except the magnetic field of the Earth which is about 50 μT, and that thus alignment of this degree cannot be considered alignment due to external magnetic fields.

In one experiment where a large density of magnetic beads ($5 \cdot 10^5$ ml^{-1}) was used, the magnetic beads gathered at the spots in the sample nearest to the poles of the external magnet (figure 17a). However, in spite of the large number of beads present to align the collagen fibrils, no alignment was found in this sample. Although there was no alignment due to the magnetic beads, there was often clear of alignment of collagen fibrils in the vicinity of air bubbles; an example of this is shown in figure 17b. The direction of this alignment does not seem directly correlated to these bubbles, but the alignment often stretched out over several hundred micrometers. Another source of alignment which introduces unwanted stress in the matrix is stretching of the network by squeezing the sample. Figure 17c shows a sample which was accidentally squeezed until some collagen solution dripped from the silicon grease sealed sides. Since there is an extension of the network mainly directed towards these sides, the collagen will be aligned in those directions, which are horizontal in this image.

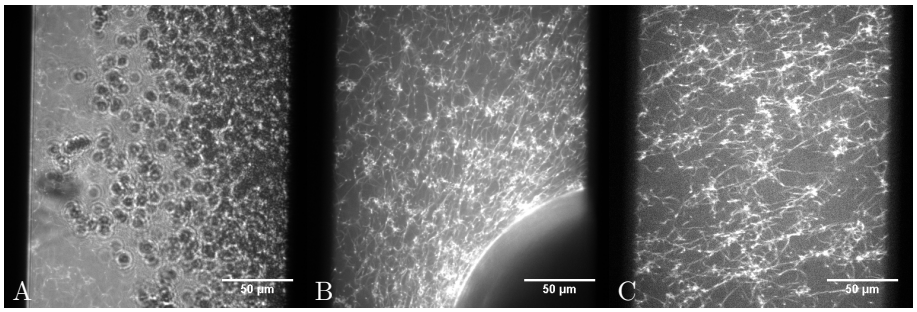

Figure 17: **A.** Many beads are gathered near one of the poles of the external magnet. **B.** Alignment caused by either an airbubble or **C.** stretching of the network.

3.4 Alignment using flow

A flow-based method to align collagen fibrils was also tried. Flows with a low Reynolds number are normally lamellar flows. In flows with a Reynolds number lower than one, the inertial forces are smaller than the viscous forces. In these flows there is no turbulence and the flow moves in lamellae. The solution in the center of the flow moves fastest, while the solution touching the confining walls does not move at all. This sets up a gradient in flow velocity. Different parts of objects in such a flow have different speeds and long objects tend to align with the flow.

To achieve flow alignment, we made a channel of 1 mm wide and 80 μm high in PDMS and covered it with a microscope slide. Polymerizing collagen was then flowed through this channel at concentrations between 0.1 and 1 mg/ml. The length of the tubes through which collagen was injected into the channel was chosen such that the collagen would be in the tubing during the lag time. In other experiments collagen was pre-polymerized before flowing through the channel. In both cases three different flow velocities resulting in shear rates of 83.3, 41.7 and 20.8 s^{-1} were used.

Flow generally did produce alignment, however, this alignment was only found at the surfaces of the flow cell. Figure 18a shows such a surface covered with stuck collagen fibrils. This alignment process likely works as follows: when a collagen fibril flows through the flow cell, one end sticks to the surface while the rest of the fibril is dragged by the fluid flow and gets aligned with it like a flag in the wind. Further away from the surface the collagen fibrils often formed large clots of unaligned collagen. In between these clots, channels formed through which the main part of the current flows (figure 18b).

3.5 Conclusion

We were not able to reproduce two previously published methods to align collagen fibrils in magnetic fields. An alternative alignment method based on flow did lead to fibril alignment, but only in a thin layer on the surface. Most of the other methods to align fibrils reported in literature (section 3.1) are unusable for us because they induce stress in the network.

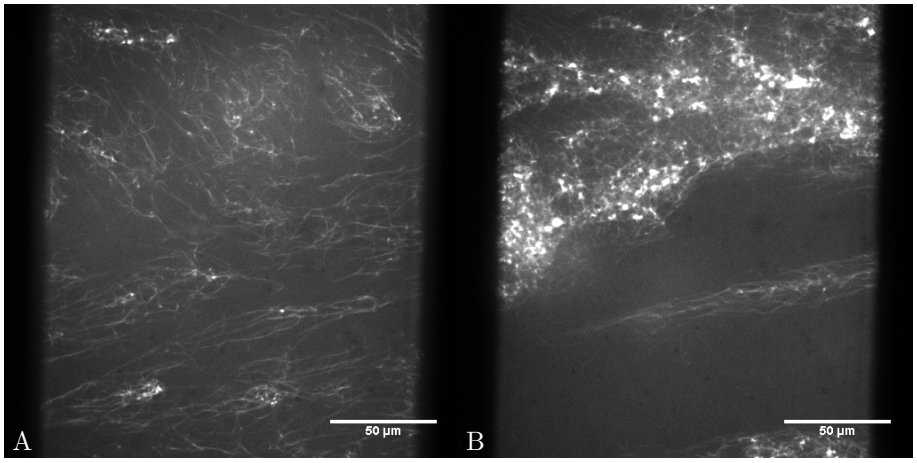

Figure 18: A. Collagen which flows and polymerizes at the same time aligns at the glass surface of the flow cell. **B.** At larger distances from the surface the collagen fibrils tend to clump together forming channels through which the fluid flows, while in the clumps there is no flow and no alignment.

4 Materials & Methods

4.1 Collagen

Collagen solutions were prepared by diluting pepsinized collagen (Nutragen, Advanced BioMatrix, 6.0 mg/ml bovine dermal collagen) at 4°C in a phosphate buffer containing 0.101 M Na_2HPO_4 (10× PB), 0.146 M NaCl and NaOH or HCl. Final solutions contained different concentrations of collagen between 0.1 and 10 mg/ml collagen in 1× PBS (PB and saline), had a pH around 7.4 (measured using a Hanna Instruments pH 211 pH-meter) and an ionic strength of 0.17.

4.2 Turbidity

Turbidimetric experiments were done using a Perkin Elmer Lambda 35 dual beam spectrophotometer with temperature control by a Perkin Elmer 6+6 peltier system. Cuvettes were prewarmed at 37°C in the spectrophotometer. The acidic collagen solution, its dilution buffer and the reference solution where degassed separately ro remove air bubbles, before the acidic collagen solution was mixed into the dilution buffer. Thereafter the solution was pipetted into the cuvettes. Cuvettes with a 10 mm (Hellma 115B-QS) or 1 mm (Hellma 105.211-QS) path length, with a volume of respectively 500 µl and 10 µl were used. The reference sample contained the same buffer but had the acidic collagen solution substituted for 0.01 M HCl. Immediately after insertion of the sample and the reference, the measurement was started. The estimated dead time between mixing and the start of the measurements is 15 seconds. For measurements of lag phases the time resolution was chosen as high as possible, which was limited by the limited number of successive measurements the photospectrometer can do. For further measurements after the lag and growth phases the Peltier unit was set to a new temperature manually, and the spectrophotometer was restarted. In some cases a C++ program was used to automatically restart the spectrophotometer (see section 5.1).

4.2.1 Lag time determination

Turbidimetric data was used to extract the length of the lag phase. Points between $\frac{1}{4}$ and $\frac{3}{4}$ of the maximum (final) turbidity (τ) value were fitted to a logarithmic function of time (t) [34]. Then the intercept on the time axis is taken as the lag time. Some authors use a linear function for the same purpose [35], these methods usually differ less than a few percent.

4.3 Confocal imaging

Samples were imaged using a spinning disk confocal microscope (Leica DM IRB inverted microscope with a Yokogawa CSU 22 spinning disk confocal scanner) with 40× and 100× objectives (PL Fluotar 40× 1.00-0.50 & PL Fluotar 100× 1.30). Depending on labelling ratio and area density of collagen in the sample, exposure times between 100 and 1000 ms were used. The Coherent Sapphire CDRH LP 488 nm LASER was almost always set to full power. To reduce noise, one image is an average of 3 or 10 successive exposures.

4.3.1 Labeling

Collagen was fluorescently labelled with HiLyte fluor 488. The labeling was carried out in a buffer of pH 7.3 containing 0.25 M $NaHCO_3$ and 0.4 M NaCl. The dye was diluted in some DMSO and then added to the collagen in the buffer, such that the ratio dye to collagen molecules was 10:1, and given twelve hours to react with the collagen. Afterwards, the labeled collagen was dialyzed back into 0.01 M HCl. Labelled and unlabelled collagen were mixed in 1:20 to 1:5 ratios.

4.3.2 Surface passivation

To reduce inhomogeneities of the network due to interactions of collagen with the microscope slide surfaces, PLL-PEG, κ-casein and pluronic f127 were used to passivate glass surfaces. 0.25 mg/ml PLL-PEG was diluted in milliQ, 0.05 mg/ml κ-casein was diluted in buffer (1× PBS) and 10% f127 was diluted in DMSO first and then mixed with 1× PBS to give a final concentration of 1%. Passivation was done by sonicating Menzel-Gläser microscope slides in 1% Hellmanex (Hellma analytics Hellmanex®II) for 20 minutes, twice in milliQ for five minutes, in 70% ethanol for 20 minutes and finally in milliQ for five minutes. Menzel-Gläser 24×24 mm #1 cover slips were sonicated in 100% isopropanol for 20 minutes, twice in milliQ for 5 minutes, in 1 M KOH for 20 minutes and finally in milliQ for five minutes. A chamber was formed by placing a cover slip on top of a microscope slide, separated by two strips of parafilm. Melting the parafilm at 120 °C attached the glasses to each other separated by a distance of about 100 µm. After that the chamber was filled with PLL-PEG, κ-casein and f127 respectively for five minutes each. Between and after these steps the glasses were washed with 1× PBS. After the collagen solution was pipetted into the chamber it was sealed with silicon grease to prevent solvent evaporation.

4.4 Image analysis

Alignment was quantified using ImageJ 1.45 software with the OrientationJ plugin [36]. OrientationJ calculates the orientation of every pixel by determining the difference in brightness between neighboring pixels. The orientation of pixels in a fibril would be in the direction in which the difference in brightness is the smallest. These orientations are weighted by the local coherency which is a value for the consistency of the orientation between neighboring pixels. Three parameters called Gaussian window σ, Min. Coherency and Min. Energy were set to respectively 5 pixels, 30% and 2%. The applied Gaussian window ensures that tiny variations in orientation within a fibril are washed out, the minimum coherency and energy which is a value for the difference in brightness between neighboring pixels, are used to separate fibrils from the background, and from clots of collagen in which a orientation is hard to determine.

4.5 Magnetic fields

To align collagen in a magnetic field, several configurations of magnets where used. Two blocks (Supermagnete Q-46-30-10-N) spaced 7 mm apart gave a field of about 0.50 T (F.W. Bell 4048 digital Gaussmeter). To achieve a higher field of about 0.66 T, several cylindrical magnets (Supermagnete S-20-10-N, S-20-05-N) where stacked on either side of this configuration. Microscope slides 6 mm wide were placed in the gap between these magnets so that the magnetic field lines would be in the plane of the glass. To do so Menzel Gläser microscope slides and cover slips were sawed in four pieces.

4.5.1 Stronger magnetic fields

An even higher magnetic field was achieved in a configuration (figure 19) of six magnets (Supermagnete Q-40-10-10-N), resulting in a one by four centimeter region with a homogeneous field of about 1.1 T. One microscope slide at a time fits in the hole between these magnets, so for some experiments slides with multiple channels were used. This configuration was found using finite element method magnetics software (femm 4.2 [37]). A planar symmetry with 4 cm depth was selected. In the space between the magnets a mesh-size of 0.1 mm was used, everywhere else the mesh-size was 1 mm. The magnets were modeled using 40 MGOe NdFeB magnetic material from the program's materials library.

4.5.2 Magnetic beads

To achieve alignment induced by moving magnetic beads through a polymerizing collagen solution [31], streptavidin coated superparamagnetic beads (Bangs Labs BM551), approximately 1.5 µm in diameter, were added to some samples and pulled through the sample by an external magnet. The magnets used

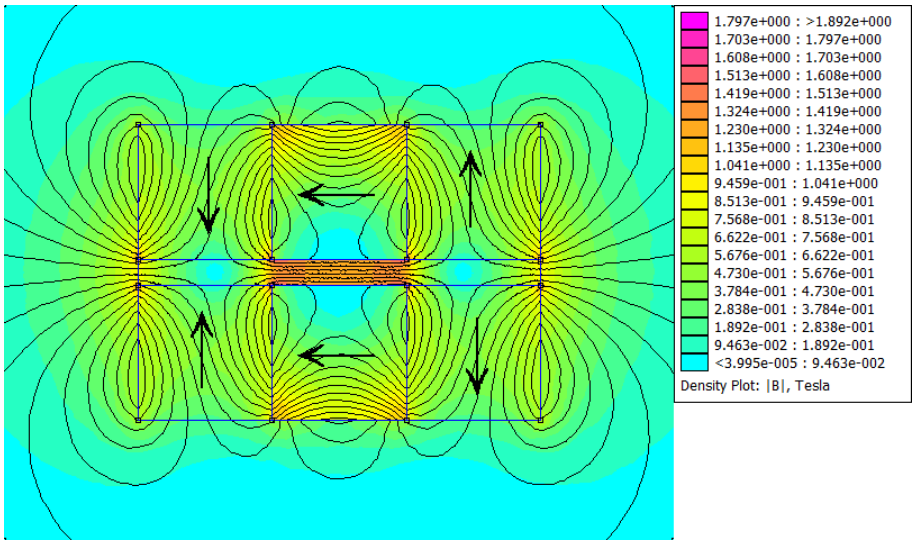

Figure 19: Side view of the magnet configuration resulting in a >1T field in the space in between. The 1 × 1 × 4 cm magnets are viewed from their 1 × 1 cm sides. Arrows depict the magnetization of the magnets, and the curved lines are magnetic field lines. (image made with femm 4.2 software)

where supermagnete S-20-10-N in experiments where this cylindrical magnet was placed besides a row of slides with collagen solution. In other experiments either supermagnete S-04-13-N or a small magnetic stir bar was used. These beads were washed and diluted in the 10× PB buffer to achieve a final concentration of 0.1 mg/ml. Washing was performed by mixing 20 µl beads in storage solution (PBS pH 7.5, 0.1% BSA, EDTA, NaN_3) with 80 µl 10× PB. This mixture was vortexed until the beads were distributed evenly in the solution. Then the beads were separated from the fluid by holding the eppendorf tube containing the mixture against a magnet (Supermagnete S-20-03-N). After this the fluid was removed, leaving the beads in the tube. Then 100 µl 10× buffer was added, vortexed and removed again, this was done 3 times after which 100 µl 10× buffer was added and we have 0.1 g beads in 100 µl 10 × PB. After insertion of the sample between microscope slide and cover slip, a cylindrical magnet (Supermagnete S-20-10-N) was placed next to the microscope slide, or a stirring magnet was placed on top of the cover slip.

4.6 Alignment by flow

4.6.1 Flow cells

Alignment also can be induced by flow [18–20, 22]. To this end, several PDMS flow cells were made. The top and sides of the cells consist of PDMS, the bottom is a cover slip. For this a mold was made in SU8 on a silicon wafer using UV photolithography. The wafer contains a negative of the channel which is approximately 1 mm wide, 1 cm long and 80 µm high. The channel gets wider and higher at the end to allow easy introduction of a needle. To enhance the rigidity of the channel a piece of cover slip was embedded in the PDMS before curing, which is visible in figure 20. After curing the PDMS was pulled from the wafer and stuck to a cover slip (Menzel 24×60 mm, #1), the needles and tubing were attached and glued with a drop of UV-glue.

4.6.2 Flow

A syringe pump (Harvard apparatus, PHD ultra syringe pump with terumo 10 ml syringe) was used to achieve a steady flow in the flow cell. Flow speeds of 1, 2, and 4 µl/min were used, resulting in shear rates ($\dot{\gamma} = 8v/h$, v is the flow velocity, $h = 80$ µm is the channel height) of 83.3 s^{-1}, 41.7 s^{-1} and 20.8 s^{-1}. In all experiments the Reynolds number ($Re = vh \cdot \rho/\mu$, ρ is the fluids density, μ is the dynamic viscosity) was below 1. Two types of flow experiments were carried out: in variant A the neutralized collagen solution was kept at 4 °C while the tubing and flow cell were kept at 37 °C. This way collagen fibers form while flowing through the tubing and the flowcell. In variant B the collagen was allowed to polymerize in a 10 ml tube at 37 °for at least a day. After that the resulting network was broken up by pumping the fluid back and forth through a syringe needle. To remove large clots the solution was centrifuged for six minutes at 1000 g. After that the supernatant was flowed through the flow cell at room temperature. After imaging on the confocal microscope the PDMS flow cell was rinsed with about 1 ml of 0.01 M HCl, ethanol and milliQ successively, and reused for up to three times. The glass coverslip attached to the PDMS channel was discarded after each measurement.

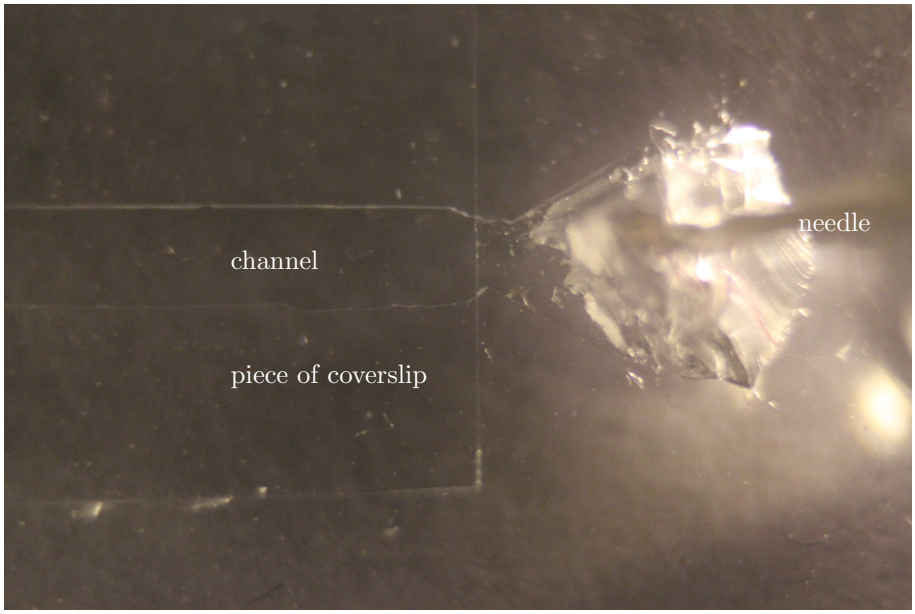

Figure 20: Photograph of a PDMS flowchamber, topview. Visible is one half of the chamber, 1 mm wide, with a piece of cover slip on top, to the right is one of the syringe needles. Underneath this is a cover slip forming the bottom of the chamber.

5 Appendix

5.1 Mouseclicker code

The following C++ code has been used to restart measurements on the spectrophotometer. It emulates a click on the left mouse button at position (x, y) from the left top corner of the program window; r times at t minute intervals. It takes these variables and the window name of the window in which is to be clicked as input.

```
#include <windows.h>
#include <ctime>
#include <iostream>

using namespace std;

void wait( int minutes ) { //check clock every 5 seconds
  clock_t endwait;
  endwait = clock () + 60 * minutes * CLOCKS_PER_SEC;
  while (clock() < endwait) {Sleep(5000);}
}

HWND findwindow( int& a, int& b, char* program ) {
  HWND window;      //get window handle and top-left coordinates
  do {
  LPCSTR p = program;
    window = FindWindow(NULL, p);
        Sleep(10);
  } while (window == NULL);
  Sleep(200);
  RECT r;
  GetWindowRect(window, &r);
  RECT cr;
  GetClientRect(window, &cr);
  a = r.left;
  b = r.top;
  return window;
}

void click( int x, int y ) { //clicks pos (x,y) rel to top-left
  for(int i = 100; i > 0; i--) { //move around a little to wake pc
    SetCursorPos(x+i,y+i);
    Sleep(20);
  }
  Sleep(2000);
  SetCursorPos(x,y);
  mouse_event(MOUSEEVENTF_LEFTDOWN, x, y, 0, 0);
  mouse_event(MOUSEEVENTF_LEFTUP, x, y, 0, 0);
}

int main(int argc, char* argv[]) {
  HWND window;
  char* program; //actually the name of the window in question
  string str;
  int x = 0, y = 0, repeats = 1, a, b, t;
```

```
46   if(argc < 3) {
47     cout << "Mouseclicker, clicks at a specific point in program at"
48          << " time-intervals. Wim Pomp, AMOLF, 29-06-2011" << endl
49          << "Usage: mouseclicker.exe -p [program] -x [x-coordinate]"
50          << " -y [y-coordinate] -r [repeats] -t [time-interval]."
51          << endl;
52     return 0;
53   }
54   for( int i=1; i < argc; i++ ) { //find parameters
55     str = argv[i];
56     if(str == "-p")
57       program = argv[i+1];
58     else if(str == "-x")
59       x = atoi(argv[i+1]);
60     else if(str == "-y")
61       y = atoi(argv[i+1]);
62     else if(str == "-t")
63       t = atoi(argv[i+1]);
64     else if(str == "-r")
65       repeats = atoi(argv[i+1]);
66   }
67   cout << "I will click " << repeats << " times on position (" << x
68        << "," << y << ") in the program " << program << " at " << t
69        << " minute intervals." << endl;
70   system("PAUSE");
71   cout << "FROM NOW ON DO NOT CLICK ANYTHING WITH THE MOUSE!"
72        << endl;
73   window = findwindow(a,b,program);  //find the handle of the window
74   click(a+x,b+y);                    //click once for starters
75   for( int i=1; i < repeats; i++ ) { //wait some time
76     wait(t);                         //and click again
77     click(a+x,b+y);                  //bis...
78   }
79   return 0;
80 }
```

References

[1] R.A. Gelman, B.R. Williams, and K.A. Piez. Collagen fibril formation: evidence for a multistep process. *The Journal of Biological Chemistry*, 254(1):180–186, 1979.

[2] G.C. Na. Monomer and oligomer of type I collagen: Molecular properties and fibril assembly. *Biochemistry*, 28:7161–7167, 1989.

[3] K.E. Kadler, D.F. Holmes, J.A. Trotter, and J.A. Chapman. Collagen fibril formation. *Biochemical Journal*, 316:1–11, 1996.

[4] Ian Streeter and Nora H. de Leeuw. A molecular dynamics study of the interprotein interactions in collagen fibrils. *Soft Matter*, 7:3373–3382, 2011.

[5] S. Leikin, D. C. Rau, and V. A. Parsegian. Direct measurement of forces between self-assembled proteins: Temperature-dependent exponential forces between collagen triple helices. *Proceedings of the National Academy of Sciences USA*, 91:276–280, 1994.

[6] Peter Fratzl. *Collagen: Structure and Mechanics*. Springer, 2008.

[7] J. Robin Harris and Andreas Reiber. Influence of saline and pH on collagen type I fibrillogenesis in vitro: Fibril polymorphism and colloidal gold labelling. *Micron*, 38:513–521, 2007.

[8] Bruce J. Berne. Interpretation of the light scattering from long rods. *Journal of Molecular Biology*, 89(4):755–758, 1974.

[9] G.C. Wood and M.K. Keech. The effect of experimental conditions: Kinetic and electron-microscope studies. *Biochemical journal*, 75:588–598, 1960.

[10] C. Yeromonahos, B. Polack, and F. Caton. Nanostructure of the fibrin clot. *Biophysical Journal*, 99:2018–2027, 201.

[11] G.C. Wood. The formation of fibrils from collagen solutions 2. A mechanism of collagen-fibril formation. *Biochemical Journal*, 75:598–605, 1960.

[12] Frederik H. Silver. Type I collagen fibrillogenesis in vitro, additional evidence for the assembly mechanism. *The Journal of Biological Chemistry*, 256(10):4973–4977, 1981.

[13] Jonathan B.L. Bard and John A. Chapman. Diameters of collagen fibrils grown in vitro. *Nature New Biology*, 246:38–84, 1973.

[14] S. Arrhenius. Uber die reaktionsgeschwindigkeit bei der inversion von rohrzucker durch sauren. *Zeitung fur Physikalische Chemie*, 4:226–248, 1889.

[15] Howard B. Bensusan and Barbara L. Hoyt. The effect of various parameters on the rate of formation of fubers from collagen solutions. *Journal of the American Chemical Society*, pages 719–724, 1958.

[16] G.C. Na, L.J. Phillips, and E.I. Freire. In vitro collagen fibril assembly: Thermodynamic studies. *Biochemistry*, 28:7153–7161, 1989.

[17] C. Yeromonahos, B. Polack, and F. Caton. Erratum concerning the nanostructure of the fibrin clot. 2011.

[18] B. Lanfer, U. Freudenberg, R. Zimmerman, D. Stamov, V. Korber, and C. Werner. Aligned fibrillar collagen matrices obtained by shear flow deposition. *Biomaterials*, 29:3888–3895, 2008.

[19] Philip Lee, Rob Lin, James Moon, and Luke P. Lee. Microfluidic alignment of collagen fibers for in vitro cell culture. *Biomed Microdevices*, 8:35–41, 2006.

[20] Nima Saeidi, Edward A. Sander, and Jeffrey W. Ruberti. Dynamic shear-influenced collagen self-assembly. *Biomaterials*, 30:6581–6592, 2009.

[21] Nima Saeidi, Edward A. Sander, Ramin Zareian, and Jeffrey W. Ruberti. Production of highly aligned collagen lamellae by combining shear force and thin film confinement. *Acta Biomaterialia*, 7:2437–2447, 2011.

[22] Yuji Tanaka, Koichi Baba, Thomas J. Duncan, Akira Kubota, Toru Asahi, Andrew J. Quantock, Masayuki Yamato, Teru Okano, and Kohji Nishida. Transparent, tough collagen laminates prepared by oriented flow casting, multi-cyclic vitrification and chemical cross-linking. *Biomaterials*, 32:3359–3366, 2011.

[23] Xingguo Cheng, Umut A. Gurkan, Christopher J. Dehen, Michael P. Tate, Hugh W. Hillhous, Garth J. Simpson, and Ozan Akkus. An electrochemical fabrication process for the assembly of anisotropically oriented collagen bundles. *Biomaterials*, 29:3278–3288, 2008.

[24] Chen Huang, Rui Chen, Qinfei Ke, Yosry Morsi, Kuihua Zhang, and Xiumei Mo. Electrospun collagen-chitosan-TPU nanofibrous scaffolds for tissue engineered tubular grafts. *Colloids and Surfaces B: Biointerfaces*, 82(2):307–315, 2011.

[25] L. Buttafoco, N.G. Kolkman, P. Engbers-Buijtenhuijs, A.A. Poot, P.J. Dijkstra, I Vermes, and J. Feijen. Electrospinning of collagen and elastin for tissue engineering applications. *Biomaterials*, 27:724–734, 2006.

[26] Scott A. Sell, Michael J. McClure, Koyal Garg, Patricia S. Wolfe, and Gary L. Bowlin. Electrospinning of collagen/biopolymers for regenerative medicine and cardiovascular tissue engineering. *Advanced Drug Delivery Reviews*, 61(12):1007–1019, 2009.

[27] D. Vader, A. Kabla, D. Weitz, and L. Mahadevan. Strain-induced alignment in collagen gels. *Plos one*, 4(6):1–12, 2009.

[28] Jiang F., Khairy K., Poole K., Howard J., and Müller D.J. Creating nanoscopic collagen matrices using atomic force microscopy. *Microscopy Research and Technique*, 64:435–440, 2004.

[29] Jim Torbet, Marilyne Malbouyres, Nicolas Builles, Virginie Justin, Muriel Roulet, Odile Damour, Ake Oldberg, Florence Ruggiero, and David J.S. Hulmes. Orthogonal scaffold of magnetically aligned collagen lamellae for corneal stroma reconstruction. *Biomaterials*, 28:4268–4276, 2007.

[30] A. Erikson, H. Nortvedt Andersen, S. Nalum Naess, P. Sikorsky, and C. de Lange Davies. Physical and chemical modifications of collagen gels: impact on diffusion. *Biopolymers*, 89(2):135–143, 2007.

[31] C. Guo and L.J. Kaufman. Flow and magnetic field induced collagen alignment. *Biomaterials*, 28:1105–1114, 2007.

[32] D.L. Worcester. Structural origins of diamagnetic anisotropy in proteins. *Proceedings of the National Academy of Sciences*, 75(11):5475–5477, 1978.

[33] Keir C. Neuman and Attila Nagy. Single-molecule force spectroscopy: optical tweezers, magnetic tweezers and atomic force microscopy. *Nature Methods*, 5(6):491–505, 2008.

[34] B.R. Williams, R.A. Gelman, D.C. Poppke, and K.A. Piez. Collagen fibril formation optimal in vitro conditions and preliminary kinetic results. *The Journal of Biological Chemistry*, 253(18):6578–6585, 1978.

[35] S. Han, D.J. McBride, W. Losert, and S. Leikin. Segregation of type I collagen homo- and heterotrimers in fibrils. *Journal of Molecular Biology*, 383:122–132, 2008.

[36] R. Rezakhaniha, A. Agianniotis, J.T.C. Schrauwen, A. Griffa, D. Sage, C.V.C. Bouten, F.N. van de Vosse, M. Unser, and N. Stergiopulos. Experimental investigation of collagen waviness and orientation in the arterial adventitia using confocal laser scanning microscopy. *Biomechanics and Modeling in Mechanobiology*, 2011.

[37] David Meeker. http://www.femm.info, 2011.

6 Acknowledgments

I would like to thank the following people:

- Gijsje Koenderink and Martijn de Wild for giving me the chance to do research in such a great place as AMOLF is. Their supervision and support during this time has been excellent.
- Jeanette Nguyen and Thomas Sokolowski for accepting me as their office mate.
- Magdalena Preciado Lopez for helping me with surface passivation.
- The lab technicians; Marjolein Kuit-Vinkenoog, Roland Dries and Vanda Sunderlikova, for familiarizing me with the lab.
- Thomas Schmidt for willing to be a supervisor representing the University of Leiden.
- The people of the biological soft matter group for letting me be a part of the group, and their fruitful suggestions, especially during group meetings.